NIH Public Access
Author Manuscript
Neuroscience. Author manuscript; available in PMC 2008 February 5.

Published in final edited form as:
Neuroscience. 2007 December 5; 150(2): 319–334.

Localization and Signaling of the Receptor Protein Tyrosine Kinase Tyro3 in Cortical and Hippocampal Neurons

Anne L Prieto[1], **Sijy O'Dell**[1], **Brian Varnum**[3], and **Cary Lai**[2]

1 *Dept of Psychological and Brain Sciences, Indiana University, Bloomington, IN*

2 *Molecular and Integrative Neuroscience Department, The Scripps Research Institute, La Jolla, CA*

3 *AMGEN Inc, Thousand Oaks, CA*

Abstract

Protein phosphorylation serves as a critical biochemical regulator of short-term and long-term synaptic plasticity. Receptor protein tyrosine kinases (RPTKs) including members of the trk, eph and erbB subfamilies have been shown to modulate signaling cascades that influence synaptic function in the central nervous system (CNS). Tyro3 is one of 3 RPTKs belonging to the "TAM" receptor family, which also includes Axl and Mer. Tyro3 is the most widely expressed of these receptors in the CNS. Despite recent advances suggesting roles for members of this receptor family in the reproductive and immune systems, their functions in the CNS remain largely unexplored. In an effort to elucidate the roles of Tyro3 and its ligand Gas6 in the hippocampus and cortex, we performed a detailed study of the localization and signaling of Tyro3 polypeptides in hippocampal and cortical neurons. Tyro3 was readily detected in dendrites and in the soma where it was distributed in a punctate pattern. Tyro3 exhibited only a limited level of co-localization with PSD-95, suggesting that while located within dendrites, it was not confined to the postsynaptic compartment. In addition, Tyro3 was also identified in the axons and growth cones of immature neurons. The prominent expression of Tyro3 in dendrites suggested that it may be capable of modulating signaling pathways triggered by synaptic transmission. We have provided evidence in support of this role by demonstrating that Gas6 induced the phosphorylation of Tyro3 in cortical neurons *in vitro*, resulting in the recruitment of the mitogen-activated protein kinase (MAPK) and the phosphoinositide-3 kinase (PI(3)K) signaling pathways. As these pathways play critical roles in the induction of hippocampal long-term potentiation (LTP), these findings suggest that Tyro3 signaling may influence synaptic plasticity in the dendritic compartment of hippocampal and cortical neurons.

Keywords

phosphorylation; dendrites; MAPkinase; Gas6; CA1; synaptic plasticity

Tyro3 belongs to the "TAM" receptor family of receptor protein tyrosine kinases (RPTKs) comprised of three receptors Tyro3, Axl, and Mer (Lemke and Lu, 2003, Hafizi and Dahlback, 2006b). These receptors have been best characterized for their roles in immune regulation

Address correspondence and reprint requests to: Anne L. Prieto, Dept. of Psychological and Brain Sciences, Indiana University, 1101 East 10th Street, Bloomington, IN 47405, USA., Telephone: (812) 855-4642, Fax (812) 855-4691, email aprieto@indiana.edu.
Section Editor (Cellular Neuroscience): Dr. Constantino Sotelo, CNRS UMR 7102, Universite Pierre et Marie Curie, 6eme etage, Bat B, Case 12, 9Quai, St. Bernard, 75005, Paris, France.

Publisher's Disclaimer: This is a PDF file of an unedited manuscript that has been accepted for publication. As a service to our customers we are providing this early version of the manuscript. The manuscript will undergo copyediting, typesetting, and review of the resulting proof before it is published in its final citable form. Please note that during the production process errors may be discovered which could affect the content, and all legal disclaimers that apply to the journal pertain.

NIH-PA Author Manuscript
NIH-PA Author Manuscript
NIH-PA Author Manuscript

NIH-PA Author Manuscript

NIH-PA Author Manuscript

NIH-PA Author Manuscript

(Lemke and Lu, 2003, Caraux et al., 2006), fertility (Lu et al., 1999), thrombosis (Angelillo-Scherrer et al., 2005) and phagocytosis (Lemke and Lu, 2003, Hafizi and Dahlback, 2006b). In the nervous sytem, Mer and Tyro3 have been implicated in the phagocytosis of receptor outer segments by retinal epithelial cells (D'Cruz et al., 2000, Hall et al., 2005, Prasad et al., 2006) and Axl appears to play a role in oligodendrocyte survival (Shankar et al., 2003, Shankar et al., 2006). However, the role of these receptors in neurons has received little attention.

Tyro3 is the primary TAM receptor detected in neurons of the CNS with *in situ* hybridization studies revealing high levels of expression throughout the cortex and in the CA1 field of the hippocampus (Prieto et al., 2000). Of particular interest is the high level of Tyro3 expression in the CA1 region, an area known to support long-term potentiation (LTP), an electrophysiological measure of synaptic strengthening thought to underlie learning and memory (Malenka and Nicoll, 1999). This pattern of expression has led us to hypothesize that Tyro3 may serve as a potential modulator of postsynaptic neuronal excitability. As there is considerable evidence that protein phosphorylation plays critical roles in regulating different stages of LTP (Thomas and Huganir, 2004) and as other RPTKs including the trk (Blum and Konnerth, 2005), eph (Pasquale, 2005) and erbB families (Huang et al., 2000, Kwon et al., 2005) have been implicated as regulators of neuronal plasticity, it is plausible that the tyrosine kinase Tyro3 may also play a role in synaptic function. This hypothesis is consistent with the reports of decreased LTP in young adult Tyro3 knockout mice (Lemke and Lu, 2003). RPTKs are activated by ligand binding, which promotes receptor dimerization and autophosphorylation (Schlessinger, 2000). This initiates a cascade of signaling events leading to both transient and permanent changes in cell state. TAMs are activated by a common ligand, the polypeptide Gas6 (growth arrest-specific gene6) (Varnum et al., 1995, Mark et al., 1996, Nagata et al., 1996). Gas6 is structurally related to protein S, a well-characterized coagulation factor with which it shares 42% identity at the amino acid level (Manfioletti et al., 1993) (for structure see Figure 1). Protein S has been reported to activate and bind to Tyro3 in an inter-specific manner (Stitt et al., 1995, Nyberg et al., 1997) although this ability has been the subject of considerable controversy (Godowski et al., 1995). Indeed, only recently has evidence emerged demonstrating that murine protein S can, in fact, activate the murine homologs of Tyro3 and Mer (Hall et al., 2005, Prasad et al., 2006).

The signaling molecules recruited upon Tyro3 activation in the CNS have not been identified and the number of known targets in non-neural cell types is limited (Hafizi and Dahlback, 2006b). In non-neural cells, 3 substrates that directly interact with Tyro3 have been identified. These include the kinase src, which has been shown to immunoprecipitate with Tyro3 (Toshima et al., 1995), the Ran binding protein RanBPM (Hafizi et al., 2005), and p85, the regulatory subunit of phosphatidylinositol 3-kinase (PI(3)K) (Lan et al., 2000). The association of p85 with Tyro3 was confirmed in NIH-3T3 cells using an EGFR/Tyro3 chimeric receptor. Although the functional consequences of the recruitment of PI(3)K by Tyro3 have not been addressed, the activation of AKT, a downstream target of PI(3)K via Axl has been shown to promote the survival of oligodendrocytes (Shankar et al., 2003, Shankar et al., 2006), GnRH-expressing neurons (Allen et al., 1999) and other cell types (Hafizi and Dahlback, 2006a, b). In addition to its roles in survival, the recruitment of AKT via PI(3)K can lead to the activation of the molecule mammalian target of rapamycin (mTOR) and its downstream target p70S6kinase (p70S6K), which functions as a critical regulator of cell growth by controlling several aspects of protein translation and ribosome biogenesis.

Tyro3 also contains a consensus binding site for the adaptor Grb2 (Songyang et al., 1993), suggesting that it may activate the ras/MAPK (mitogen-activated protein kinase) pathway via the ras exchange factor, an event that typically leads to activation of the MAP kinases ERK 1 and 2 (Pearson et al., 2001). Outside of the nervous system Gas6 has been previously shown to induce ERK1/2 phosphorylation in mature mouse osteoclasts (Katagiri et al., 2001). In

NIH-PA Author Manuscript

NIH-PA Author Manuscript

NIH-PA Author Manuscript

neurons, the MAPK pathway can be activated by growth factors acting through RPTKs, as is the case for the neurotrophins. The MAPK pathway has been shown to regulate gene transcription in neurons by activation of the transcription factors CREB and ELK-1. CREB activation occurs downstream of the RSK (ribosomal S6 kinase) and the MSK (mitogen and stress-activated kinases) kinases (Xing et al., 1996, Arthur et al., 2004), while Erk1 and 2 can directly phosphorylate the transcription factor ELK-1 (Hipskind et al., 1991).

In order to elucidate the functions of Tyro3 and its ligand Gas6, we have determined the subcellular localization of Tyro3 in hippocampal and cortical neurons and initiated the characterization of its signaling properties in the CNS. We have determined that although Tyro3 is expressed in the dendritic compartment of most neurons, it appears to be primarily located outside of the synapse. We have also demonstrated that Gas6-mediated activation of Tyro3 resulted in the recruitment of multiple components of both the MAPK and PI(3)K signaling pathways. These results suggest that Tyro3 is well positioned to regulate signaling pathways known to serve as critical regulators of hippocampal LTP.

Experimental Procedures

Antibodies and reagents

Recombinant human Gas6 was obtained from Amgen Inc. (Thousand Oaks, CA). Antibodies were obtained from the following sources: anti-phospho (p) ERK1/2, anti-pCREB, anti-pAKT, anti-pp70S6kinase, anti-pRSK90, and anti-pmTOR from Cell Signaling Technology (Danvers, MA); anti-phosphotyrosine (ptyr) PY99 and PY20 from Santa Cruz Biotechnology (Santa Cruz, CA); anti-GFAP, anti-04, and anti-tau from Chemicon (Temecula, CA); anti-MAPK and anti-actin from Sigma-Aldrich (St. Louis, MO); anti-PSD95 from Affinity Bioreagents (Golden, CO); anti-synaptophysin from Roche (Indianapolis, IN); anti-Grb2 from BD Biosciences (San Jose, CA); anti-β-tubulin III from Covance (Berkeley, CA); anti-CNPase from Sternberger (Lutherville, MD); Alexa Fluor 594 goat-antimouse and Alexa Fluor 488 goat-anti-rabbit from Invitrogen (Carlsbad, CA); and horse radish peroxidase (HRP) conjugated goat anti-rabbit IgG and goat antimouse IgG from Pierce (Rockford, IL). The anti-GAD-6 monoclonal antibody specific against GAD-65 was developed by David Gottlieb (Washington University St. Louis, MO). It was obtained from the Developmental Studies Hybridoma Bank developed under the auspices of the NICHD and maintained by The University of Iowa, Department of Biological Sciences.

Fusion proteins

Glutathione-S-transferase (GST) fusion proteins encoding the first and second Ig-like domains (Ig1–2) and the first and second FN-type III repeats (FN1–2) of Tyro3 were generated for use as antigens in the production of Tyro3 specific antibodies. Polymerase chain reaction (PCR) was used to amplify regions corresponding to the Ig-like domains (base pairs 317 to 838) and FN1–2 repeats (base pairs 844 to 1,453) from murine Tyro3 cDNA clone 18A (accession number X78103) (Lai et al., 1994). The PCR primers also included EcoRI and XhoI restriction sites, which were introduced at the 5' and 3' ends respectively. After EcoRI/XhoI cleavage, the PCR products were subcloned into the pGEX-4T-1 vector (Amersham Biosciences/GE Healthcare, Pittsburgh, PA). After verification of the nucleotide sequences, the recombinant constructs (Ig1–2-pGEX-4T or FN1–2-pGEX-4T) or the unmodified pGEX-4T vector were transformed into NM522 bacteria (Stratagene, La Jolla CA) and used for fusion protein production and purification as previously described (Prieto et al., 1999).

Purification of Tyro3 antibodies

Tyro3 antisera (#3488) directed against the second Ig1–2GST and FN1–2GST fusion proteins were raised in rabbits (New Zealand White, Myrtle's Rabbitry, Thompson's Station, TN) by

NIH-PA Author Manuscript

NIH-PA Author Manuscript

NIH-PA Author Manuscript

subcutaneous injection of a mixture containing 0.5 mg of purified Ig1–2GST and FN1–2-GST fusion proteins in complete Freund's adjuvant, followed by booster injections in incomplete Freund's every 2–3 weeks (Prieto et al., 2000). The immunization procedure for all other experiments in which animals were involved followed guidelines established by the NIH *Guide for the Care and Use of Laboratory Animals* and a protocol approved by the Indiana University Institutional Animal Care and Use Committee. Anti-Ig1–2 and anti-FN1–2 antibodies were affinity-purified by passing the 3488 serum sequentially through GST, Ig1–2GST and FN1–2GST-Sepharose 4B columns (Amersham Biosciences) prepared as previously described (Prieto et al., 1999). For affinity purification, serum 3488 was pre-cleared by centrifugation at 5,000g for 20 min at 4°C, diluted 1:10 with TBS (0.010 M Tris-HCl, pH 7.5 and 0.05 M NaCl) and mixed with GST/Sepharose for 1 hr at room temperature to remove the anti-GST antibodies. The eluate was then passed sequentially through an Ig1–2 GST/Sepharose column and a FN1–2GST/Sepharose column. After washing with at least 10 column volumes of TBS, the bound antibodies were eluted with 0.1M NaCl and 0.1M glycine (pH 2.5), and neutralized with 3M Tris-HCl (pH 8.9). Fractions containing the highest protein levels were analyzed for the presence of light and heavy chains by SDS-PAGE, and the immunoreactivity of the antibodies was tested by Western blot analysis as described below.

Cell culture

Rat2 cells and Rat2/T3 cells were provided by Drs. M. Gore and G. Lemke (Lai et al., 1994) and were used to test the 3488 sera and the affinity-purified antibodies. The Rat2 and Rat2/T3 cells lines were grown in Dulbecco Modified Eagle's Minimal Essential Medium (DMEM) containing 10% fetal calf serum (FCS) (Omega Scientific, Tarzana, CA), 2 mM L-glutamine, penicillin (100 U/ml) and streptomycin (100 μg/ml) (all from Invitrogen). The cell extracts used to test the antibodies were prepared as described in the section "Gas6 and glutamate activation".

Primary hippocampal and cortical neuronal cultures were prepared essentially as described by Banker *et al* (Banker, 2002). The procedures for obtaining the cortical and hippocampal cells from rat embryos followed the guidelines established by *the NIH Guide for the Care and Use of Laboratory Animals* and by a protocol approved by the Indiana University Institutional Animal Care and Use Committee. The hippocampal and cortical tissues were dissected from Sprague Dawley rat brains (Harlan Sprague Dawley Inc, Indianapolis IN) of embryonic (E) day 17–18 in Ca^{2+}/Mg^{2+}-free Hank's Balanced Salt Solution (HBSS) supplemented with 10 mM HEPES (pH 7.5)/1 mM sodium pyruvate (buffered Hank's) during the dissection (all from Invitrogen). The tissues were incubated for 20 min in 0.25% trypsin (Invitrogen) in buffered Hanks's at 37°C, washed 5 times with buffered Hank's, and dissociated using fire polished Pasteur pipettes until a single cell suspension was obtained. The cells were diluted with 5 volumes of HBSS/1.5 mM $CaCl_2$/0.5 mM $MgCl_2$ and centrifuged at 200 x g for 5 min. The cells were resuspended in Neurobasal media supplemented with B-27 (Invitrogen), 0.5 mM L-glutamine (Invitrogen) and 0.025 μM L-glutamate (Tocris Biosciences, Ellisville, MO) (Brewer et al., 1993) and seeded onto 250 μg/ml poly-L-lysine (Sigma-Aldrich, St Louis, MO) coated tissue culture plates or glass coverslips (Fisher Scientific, Fairlawn, NJ) depending on whether they were cultured for biochemical or immunocytochemical experiments. Half of the media was replaced every 4 days with media having no added glutamate, effectively decreasing the concentration of glutamate by a factor of 2 every 4 days. The cells were cultured for 1–21 days depending upon the experiment.

Gas6 activation

Neurons plated at a density of $2x10^6$ cells/60mm well were grown for 7–15 days in the media described above. The cells were treated with various concentrations of Gas6 (0–600 ng/ml) for different periods of time prior to harvesting. The activation was stopped by washing 3 times

NIH-PA Author Manuscript

NIH-PA Author Manuscript

NIH-PA Author Manuscript

with cold PBS, and the cells were harvested by scraping the wells in the presence of lysis buffer containing 50 mM Tris-HCl (pH 7.5), 150 mM NaCl, 0.1% SDS, 1% Triton X-100, 0.5 % Nonidet P-40, 0.5 mM EDTA (pH 8.0), 10 mM NaF, 2 mM Na_3VO_4, and 5mM $Na_4P_2O_7$. The buffer was supplemented with phosphatase inhibitor cocktails I and II (Sigma) and the Complete Protease Inhibitor cocktail (Roche) in concentrations suggested by the manufacturers. The cell lysates were incubated on ice for 30 min and centrifuged for 15 min at 16,000 rpm (Eppendorf, Hamburg Germany). The protein concentrations of the supernatants were determined using Bio-Rad *Dc* protein determination reagents (Bio-Rad Laboratories, Hercules, CA) and the lysates were used in the Western blotting analyses.

Fc-receptor body inhibition

Tyro3 Fcs encompass the extracellular portion of Tyro3 fused to the Fc region of the Ig molecule. To deplete Gas6 from the media, 0 or 225 ng/ml of Gas6 were preincubated with 1 μg of Tyro3 Fcs for 30 min before activation. This mixture was then used to activate Tyro3 in cortical neurons for 10 min, followed by cells lysis as described above under "Gas6 activation".

Immunoprecipitations and Western blotting

For the immunoprecipitation of Tyro3 from neuronal extracts, equivalent amounts of protein were incubated overnight at 4°C with 2 μg of affinity-purified FN2 Tyro3 antibody (Prieto et al., 2000) and 30 μl of a 1:1 Protein A-Sepharose CL-4B bead/lysis buffer slurry (Amersham Biosciences). The samples were washed 4 times with cold lysis buffer and the pellet was resuspended in 30 μl of 2X Laemmli sample buffer and heated at 98°C for 5 min prior to SDS-PAGE. Western blotting was performed as previously described, using 8% or 4–20% gradient Tris-glycine gels (Invitrogen). After electrophoresis, the proteins were transferred to Immobilon P membranes (Millipore, Billerica, MA) and blocked for 30 min at room temperature. The blocking buffer used consisted of 10mMTris-HCl (pH7.5), 150 mM NaCl and 0.1% Tween-20 (TBST) and 3% skim milk (Carnation, Nestle, Vevey Switzerland) to detect non-phosphorylated proteins, or consisted of 1% BSA (Fisher), TBST and 10 mM NaF, 2 mM Na_3VO_4, and 5 mM $Na_4P_2O_7$, to detect phosphorylated proteins. The membranes were incubated overnight at 4°C in the presence of primary antibody. The following antibodies were used for the Western blot analyses: anti-Tyro3 serum #3488 (1:1,700 dilution), anti-Tyro3 serum #5424 (1:3,500 dilution), affinity-purified anti-Ig1–2 (2.5 μg/ml), and affinity-purified anti-FN1–2 (2.5 μg/ml), affinity purified anti-FN2 (2.5 μg/ml), anti-Tyro3IgFN mix consisting of affinity purified anti-Ig1–2 (1.5 μg/ml), FN1–2 (1 μg/ml) and FN2 (2.5 μg/ml), a 1:1 mixture of anti-pTyr PY99 and PY20 (1:3,500), anti-pERK1/2 (1:1,000), anti-pCREB (1: 1,000), anti-pAKT (1:1,000), anti-pp70S6kinase (1: 1,000), anti-pRSK90 (1: 1,000), anti-pmTOR (1: 1,000), antiTUJ1 (1:3,500) and anti-Grb2 (1:500).

For preabsorption, the antibodies were resuspended in 200 μl of blocking buffer and incubated for 4 hrs at room temperature in the presence of the GST fusion proteins antigens. Serum #3488 (6 μl) was preabsorbed with a mixture of Ig1–2GST (20 μg) and FN1–2GST (10 μg); affinity purified anti-Ig1–2 (2.5 μg/ml) was preabsorbed with Ig1–2GST (20 μg); affinity purified anti-FN1–2 (2.5 μg/ml) was preabsorbed with FN1–2GST (10 μg); affinity purified anti-FN2 (2.5 μg/ml) was preabsorbed with FN2GST (20 μg); anti-Tyro3IgFN mix was preabsorbed with a mixture of Ig1–2GST (10 μg), FN1–2GST (20 μg), and FN2GST (20 μg). Following the incubation period the mixture was diluted to 10 mls with blocking buffer and used to blot the membranes.

After the overnight incubation with the primary antibodies the membranes were washed 5 times for 5 min each with TBST, blocked for 15 min as described above, and then incubated for 60 min with either HRP- goat anti-rabbit IgG or HRP-goat antimouse IgG (at 1:10,000). The blots were washed 5 times for 5 min with TBST and processed using chemiluminescent detection

NIH-PA Author Manuscript

NIH-PA Author Manuscript

NIH-PA Author Manuscript

with the Super Signal West Pico Chemiluminescent Substrate ECL system (Pierce) according to instructions provided by the manufacturers.

Antibody membrane stripping

The membranes were hydrated for 15 min in TBST, and then incubated for 30 min at 56°C in a solution containing 100 mM 2-mercaptoethanol, 62.5 mM Tris-HCl pH 6.8, and 2% SDS. The membranes were then washed 10 times for 15 min in TBST to completely remove the 2-mercaptoethanol, and then blocked for 1 hr in the milk-containing blocking buffer described above. Following this treatment the membranes were reblotted using the same procedure as previously described.

Western Blot quatititation

After antibody detection using chemiluminescence (Pierce), the membranes corresponding to immunoprecipitations were stripped of anti-pTyr antibodies and reblotted with anti-Tyro3 antibodies (5424 serum (Lai et al., 1994)). The membranes corresponding to Western blots of pAKT, pERK1/2, pRSK, pCREB, pmTOR and pp70S6K were also blotted with anti-tubulin for use as a loading control. Densitometry band measurements were obtained from the X-ray films using ChemiImager 4000 software (Alpha Innotech, San Leandro, CA) and the NIH Image 1.6 program. The densitometry ratios between anti-phosphotyrosine/anti-Tyro3 bands and the pAKT, pERK1/2, pRSK, pCREB, pmTOR and pp70S6K/tubulin bands were used to calculate relative levels of phosphorylation as shown in Figs. 6 and 7. The values are represented as percent increases from the baseline level, determined in the absence of Gas6 activation or 0 min time point depending on the experiment. Densitometry data were analyzed statistically using the 2-tailed paired sample Student's *t*-test (n = 3–4 per data set).

Tyro3 transfected cells

Rat2 untransfected cells were obtained from ATCC (American Tissue Culture Collection) and Rat2/Tyro3 transfected cells were obtained from Dr. Greg Lemke form The Salk Institute. The transfection and selection procedure to obtain these cells was previously described in Lai et al (Lai et al., 1994). Detergent extracts from both Tyro3 transfected and untransfected cells were prepared as described under "Gas6 activation" and the protein determination assay, and Western blotting was performed as described in the section "Immunoprecipitations and Western blotting".

Immunohistochemistry

Adult Sprague-Dawley rats of 52 days (Harlan Sprague Dawley Inc.) were anesthetized and then transcardially perfused for 5 min with 0.1M PB (pH 7.2) (PBS lacking NaCl) followed by 4% paraformaldehyde in PB for 20 min. The tissues were equilibrated successively in 12%, 16% and 18% sucrose in PBS for cryoprotection and then frozen in dry ice. Cryostat sections of 10μm were collected onto chrom-alum coated slides and blocked for 1 hr with blocking buffer consisting of 5% goat serum (Colorado Serum, Denver, CO), 5% fetal calf serum (FCS) (Omega Scientific), PBS and 0.1% Triton X-100. Prior to staining (below), the fixed sections were washed 3 times with PBS for 10 min each. The 3488 serum (1:200) or antibody or the preabsorbed serum was diluted in blocking buffer, applied to the tissue sections, and incubated overnight at 4°C. The sections were then washed 5 times for 5 min each in 1 % goat serum and PBS and blocked as above for 30 min. The antibody was visualized using the Vector Elite ABC kit (Vector Laboratories, Burlingame, CA). The tissue sections were incubated in blocking buffer containing biotinylated goat-anti rabbit (1:200) for 45 min. They were then washed 3 times for 10 min each in PBS and incubated for 45 min with precomplexed biotinylated enzyme (Reagent B)–AvidinDH (Reagent A) at half the concentration suggested by the manufacturers. The sections were washed twice for 10 min in PBS and once for 10 min in PB. A colorimetric

NIH-PA Author Manuscript

NIH-PA Author Manuscript

NIH-PA Author Manuscript

reaction using the diaminobenzidine (DAB)-peroxidase reaction was performed per the manufacturer's instructions.

Immunocytochemistry

Primary neurons were seeded and grown on 12 mm glass coverslips (Fisher Scientific) coated with 250 μg/ml of poly-L lysine (Sigma-Aldrich) and were fixed with cold 4% paraformaldehyde/4% sucrose in PBS for 30 min. The fixative was removed by washing 3 times for 10 min with cold PBS. The cells were then processed for immunofluorescent staining. For this, the coverslips were blocked for 1 hr with blocking buffer either containing detergent (as described above in the "Immunohistochemistry" section) or omitting the 0.1% Triton-X100 (blocking buffer minus detergent).

The primary antibodies were diluted in blocking buffer with or without 0.1% Triton X-100 and applied to the cells or tissue sections and incubated overnight at 4°C. The following antibodies were used: serum #3488 (1:200), anti-Tyro3IgFN (a mixture of affinity purified anti-Ig1–2 (1.5 μg/ml) , FN1–2 (1μg/ml) and FN2 (2.5 μg/ml), anti-GFAP (1:500), anti-synaptophysin (1:200), anti-actin (1:500), anti-PSD95 (1:300), anti-O4 (1:200), anti-tau (1:200), anti-TuJ1 (1:500), anti-CNPase (1:1000) and affinity-purified anti-GAD-6 (1:200). After incubation with the primary antibody, the cells were washed 5 times for 5 min each in PBS/1% goat serum and blocked as above for 30 min. The tissue sections and cells were incubated for 60 min with Alexa 488-labeled goat-anti-rabbit antibodies (for the anti-Tyro3 antibodies) and Alexa 594-labeled goat-antimouse antibodies (1:300 dilution) for the monoclonal antibodies. The coverslips were then washed once for 5 min in 1% goat serum and PBS and incubated for 30 minutes in PBS/10 μg/ml 4'-6-diamidino-2-phenylindole (DAPI, Roche) to visualize and count the nuclei of all the cells present in the culture. The coverslips were further washed 5 times for 5 min washes in PBS/1% goat serum and were mounted onto glass slides using Vectashield (Vector Laboratories). The cells were photographed under epifluorescence, with immunofluorescence staining considered to be at background levels when the intensity of the signal (very low) matched that observed when only secondary antibodies were used. Images were acquired using a Nikon E800 microscope equipped with a Hamamatsu Orca ER digital CCD camera or with a Nikon TE2000 inverted microscope and BD CARVII White light confocal imaging system equipped with a Cascade 16 bit CCD camera. The images were generated using the Universal Imaging Corporation Metamorph 6.1 software package. Images were not modified other than relative adjustments of levels, brightness, contrast and magnification.

Cellular composition

To determine the cellular composition of the neuronal cultures, we used a morphological and quantitative approach by using antibodies that distinguished the different cell types. Neurons were identified using the TuJ1 antibody that recognizes β-tubulinIII, oligodendrocytes were identified with the anti-CNPase antibody that recognizes the 2', 3' cyclic nucleotide 3'-phosphodiesterase, and astrocytes were detected using an antibody that recognizes the glial fibrilliary acidic protein (GFAP). The nuclei of the cells were also labeled with DAPI.

A selection of 4 different coverslips containing hippocampal cultures of 12 days *in vitro* (DIV) from 2 independent cell preparations (8 total) (Preparation 1 and 2) were stained with either anti-CNPase or anti-GFAP. The total number of CNPase-positive and GFAP-positive cells were counted for each coverslip. The total number of cells was calculated by averaging the number of DAPI-positive nuclei in 8 randomly chosen fields from each coverslip. The total number of cells on the coverslip was calculated by multiplying this number by the total area of the coverslip.

NIH-PA Author Manuscript

NIH-PA Author Manuscript

NIH-PA Author Manuscript

Results

Characterization of Antibodies Directed Against Extracellular Epitopes in Tyro3

In order to identify the sites of Tyro3 expression in tissue sections and isolated neurons, two different anti-Tyro3 sera were utilized, one serum recognizing the second fibronectin (FN2)-type III repeat (#2782) (Prieto et al., 2000) as well as a new antiserum (#3488) prepared against an antigen mixture containing both the immunoglobulin (Ig) and FN-type III domains (see Fig. 1 and Experimental Procedures section). In addition to these sera, 2 distinct affinity purified fractions of serum #3488 were also prepared that specifically recognized either the Ig- or FN-type III domains ("anti-Ig1–2" and "anti-FN1–2" respectively). We have also utilized an affinity-purified version of serum #2782 (anti-FN2) which recognizes the second FN-type III domain (Prieto et al., 2000). The specificity of these antibodies was demonstrated by testing their ability to recognize Tyro3 by Western blotting (Fig. 2A and 2B) using detergent extracts prepared from Rat2 untransfected (lane U), Tyro3 transfected Rat2 cells (Rat2/T3) (lane T) (Lai et al., 1994), and cortical brain extracts (lane C). The antisera #3488 detected a band of approximately 120 kDa in the cortical brain extracts and a doublet of approximately 125 kDa and 110 kDa in the Rat2/T3 cells (lane T) but not in the untransfected cells (lane U) (Fig. 2A panel 1). This pattern is consistent with that observed for Tyro3 using 2 previously characterized sera, #5424 and #2782 (Prieto et al., 2000). The detection of the 120 kDa band in the cortical extracts and the 125/110 kDa bands in the Rat2/T3 cells was eliminated by preincubation with a mixture of the Ig1–2GST and FN1–2GST proteins (Fig. 2A panel 2). It should be noted that bands of approximately 40 and 30 kDa in the Rat2 and Rat2/T3 fibroblasts, as well as a band of 45 kDa in the cortical extracts were not eliminated by the pre-incubation step (compare Fig. 2A panel 1 and panel 2)

In order to eliminate the non-specific immunoreactivity and obtain antibodies that selectively recognized either the Ig1–2 (Fig. 2B panels 1 and 2) or FN1–2 domains (Fig. 2B panels 3 and 4), affinity purification of serum #3488 was performed as described in the Experimental Procedures. The anti-Ig1–2 and the anti-FN1–2 affinity purified antibodies specifically recognized the 125 kDa and 110 kDa bands in the Rat2/T3 cells and the 120kDa band in the cortical extracts (Fig. 2B panels 1 and 3 respectively), as detection of these bands was blocked by preincubating the antibodies with the corresponding antigens (panels 2 and 4, respectively). In addition a series of immunoreactive protein products ranging in size from 80 and 65 kDa was observed for both affinity-purified antibodies (see Fig. 2B panels 1 and 3). These proteins were detected only in the Tyro3 transfected cells, and as their detection was blocked by pre-absorption, they represent Tyro3-specific products. A similar pattern was obtained using a distinct affinity-purified antibody (anti-FN2) derived from serum #2782 (see Fig 2B panels 5 and 6).

As we have utilized a mixture of the affinity-purified anti-Ig1–2, anti-FN1–2 and anti-FN2 antibodies (the mixture is referred to as "anti-Tyro3IgFN") for the subcellular localization studies of Tyro3 (see below), we also evaluated this combined reagent by Western blotting (Fig. 2A panels 3 and 4). This mixture detected the presence of the 125 kDa and 110 kDa bands in the Rat2/T3 cells and the 120kDa band in the cortical extracts. It also readily detected the products observed between 65 and 80 kDa and, in addition, was able to reveal a novel band of approximately 50kDa. It should be noted that all of these bands were specific to the transfected cells and all could be eliminated by preabsorption. Therefore, the anti-Tyro3IgFN antibody mixture appears to be specific for Tyro3.

Localization of Tyro3 Polypeptides in the Cerebral Cortex and Hippocampus— At the RNA level, Tyro3 has been shown to be widely expressed throughout the adult rat cortex and in pyramidal cells in the hippocampus but has not been studied at the protein level (Prieto et al., 2000). In order to evaluate the distribution of this polypeptide in the cortex and

NIH-PA Author Manuscript

NIH-PA Author Manuscript

NIH-PA Author Manuscript

hippocampus, immunohistochemical analyses were performed using antiserum #3488 on coronal sections of adult rat brain. The antiserum #3488 was tested to determine if it was suitable for immunohistochemical analyses by preabsorbing with Ig1–2GST and FN1–2GST (Fig. 3B and F). As shown by Western blotting (see Fig. 2A panel 1 and 2) this eliminated the Tyro3 immunoreactivity but did not eliminate 2 bands of approximately 40 and 30 kDa. When tested on tissue sections, as shown for cortex (Fig. 3B) and hippocampus (Fig. 3F), the immunoreactivity of this antibody was almost completely eliminated, with little or no staining detected. Given its specificity in recognizing Tyro3 and its low levels of background staining, this antibody was selected to assess Tyro3 expression in tissue sections.

As shown in Fig. 3A, Tyro3 is expressed in neurons of all cortical layers (layers II through VI) in agreement with the distribution of Tyro3 mRNAs in the cortex (Prieto et al., 2000). At the subcellular level, Tyro3 is present in the soma and in the dendritic compartment of neurons throughout the cortex (Fig. 3A, C and D). This is readily discerned in the higher magnification images of pyramidal neurons shown in panels C and D. The reduced staining detected in the intracellular portion of the dendrites is consistent with the extracellular location of the epitopes against which the antibodies were raised.

This antiserum (#3488) was also used to evaluate the distribution of Tyro3 polypeptides within the hippocampus (Fig. 3E-H). Previous *in situ* hybridization experiments have shown that the predominant site of Tyro3 mRNA expression in the hippocampus is subfield CA1 with lower levels detected in subfield CA3 (Prieto et al., 2000). As shown in Figs. 3E and G, Tyro3 polypeptides are expressed at high levels in CA1 neurons and are detected both in the soma and dendrites of pyramidal neurons. Tyro3 is also expressed in CA3 neurons, however it is not observed at significant levels in area CA2 (Fig. 3H), a pattern consistent with previous *in situ* hybridization studies (Prieto et al., 2000, Lein et al., 2004). The localization of Tyro3 to the dendritic compartment of CA1, CA3 and cortical neurons raises the interesting possibility that Tyro3 functions in the postsynaptic compartment of these neurons *in vivo*.

Localization of Tyro3 in Primary Cortical and Hippocampal Neurons *in vitro*

The subcellular distribution of Tyro3 was assessed using hippocampal and cortical cultures isolated from E17–18 rats. These cultures were primarily composed of glutamatergic neurons and GABAergic neurons. The cortical neurons were also used to identify the signaling pathways activated by this receptor. The culture conditions utilized have been shown to maintain many of the morphological characteristics and functional properties of these neuronal populations (Banker, 2002).

To determine the cellular composition of our cultures, antibodies specific for either astrocytes (GFAP), oligodendrocytes (CNPase) or neurons (TuJ1) were utilized in immunohistochemical analyses. At 12 days *in vitro* (DIV), at least 99% of the cells in our hippocampal and cortical cultures were positive for the neuronal marker, TuJ1. In contrast, only a very small percentage of cells in the cultures stained for either CNPase (0.06 and 0.04% from 2 preparations of hippocampal neurons) or GFAP (0.32% and 0.75% from the same preparations). The ratio of astrocytes to oligodendrocytes was approximately 10:1. Given the limited number of glia present in these cultures, the biochemical studies performed utilizing them should reflect the events occurring in neurons.

In order to determine the subcellular localization of Tyro3, a mixture of affinity purified anti-Ig1–2, anti-FN1–2 and anti-FN2 antibodies (anti-Tyro3IgFN) was utilized. This mixture provided staining superior to that observed for the individual antibodies. As shown in Fig. 4A, B, B', C, D, D' and E, the observed Tyro3 immunoreactivity was punctate and distributed over the entire cell surface, including the cell body, dendrites and axon. The punctate staining pattern

NIH-PA Author Manuscript

NIH-PA Author Manuscript

NIH-PA Author Manuscript

was present both in immature neurons (1 DIV, Fig. 4A and D) as well as in more differentiated neurons (5, 7 and 20 DIV, Fig. 4E, B and C, respectively).

These images primarily reflect Tyro3 extracellular staining as the antibodies recognize extracellular epitopes and the cells were not permeabilized with detergents (Fig 4A, B, B', and D). The intensity of the punctate staining was significantly decreased when Triton-X100 (0.1%) was used to permeabilize the cells as is required for optimal staining with antibodies detecting MAP2 (not shown), tau (Fig. 4E), PSD-95 (Fig. 4C), GAD-65 (Fig. 5B), O4 (Fig. 5E), and GFAP (Fig. 5H). In view of the punctate staining of Tyro3 in dendrites and axons, we sought to determine if Tyro3 is expressed in the postsynaptic compartment. A double-immunofluorescent staining analysis of hippocampal cultures (15–21 DIV) was performed using anti-Tyro3IgFN and antibodies specific for PSD-95, a protein enriched in postsynaptic densities (Sheng and Kim, 2002). As observed in the pyramidal neurons in the sections shown in Fig. 3, Tyro3 was also detected in the dendritic compartment in neurons *in vitro* (Fig. 4B and C). Although Tyro3 is present throughout the dendritic compartment, staining for this receptor exhibited only limited overlap with PSD-95 (Fig. 4C, see arrows), suggesting that it is not enriched at postsynaptic densities.

Tyro3 was also detected in axons, as evidenced by co-localization with the microtubule associated protein, tau, which preferentially localizes to this compartment (Fig. 4D and E, see arrows). Tyro3 staining was observed in neurites labeled with tau, where it was detected throughout the length of the axonal process (Fig. 4E). In addition, Tyro3 was also detected at the core and periphery of the growth cone in immature neurons (see arrow pointing to gc Fig. 4D and D').

CNS Cell Types Expressing Tyro3

Tyro3 is expressed in the vast majority of cells in hippocampal and cortical cultures, which, as previously described, contain very few glia. Although the predominant cellular phenotype is that of a large, pyramidal-shaped neuron, these cultures also contain cells that are likely to be interneurons (Benson et al., 1994). In order to determine if Tyro3 immunoreactivity was present in GABAergic neurons or in glia, double-label immunocytochemical analyses were performed using anti-Tyro3IgFN and antibodies to specific markers present on GABAergic neurons, astrocytes and oligodendrocyte precursors. To identify inhibitory neurons, the monoclonal antibody GAD-6 was used to detect GAD-65 (glutamic acid decarboxylase), an enzyme enriched in the presynaptic terminals of primarily GABAergic inhibitory neurons (Benson et al., 1994). As shown in Fig. 5C, a subset of neurons staining for Tyro3 (Fig. 5A) also stains with anti-GAD-65 (Fig. 5B), indicating that Tyro3 is expressed in inhibitory GABAergic neurons. As observed in Fig. 5C, Tyro3 is also expressed in large pyramidal neurons that lack GAD-65 staining. This cell type represents the predominant species in the TUJ1-positive population. As shown in Fig. 5F, Tyro3 is expressed in O4-positive cells (Fig. 5D-F) in these cultures as well as GFAP-positive cells (Fig. 5G-I). This confirms previous immunohistological observations (Prieto et al., 2000) indicating that Tyro3 is also expressed in CNS glial cells and that its expression is preserved in dissociated CNS cultures.

Gas6-Induced Tyro3 Phosphorylation in Cortical Cultures

To identify the signaling pathways mediated by the activation of Tyro3, the ability of Gas6 to induce Tyro3 receptor phosphorylation in cortical cultures was evaluated (Fig. 6A, A' and B). The phosphorylation levels of Tyro3 reached their maximal levels at concentrations of 90 ng/ml (1.5 nM) (Fig. 6A'') when activated for 10 min. In Figure 6A', the ability of relatively low levels of Gas6 (from 0 to 150 ng/ml) to activate Tyro3 was evaluated. In this experiment, the cells were exposed to the ligand for 5 minutes as opposed to the 10 minutes used in Figure 6A. As can be observed, the extent of Tyro3 phosphorylation is dependent upon the concentration

NIH-PA Author Manuscript

NIH-PA Author Manuscript

NIH-PA Author Manuscript

of Gas6. The nanomolar concentrations of Gas6 required to activate Tyro3 in our studies are in agreement with those reported for human Tyro3 (Rse) (Mark et al., 1996).

The time course of Tyro3 phosphorylation upon addition of 225 ng/ml Gas6 was also determined (Fig. 6B and B'). Tyro3 phosphorylation was rapidly induced, with significant receptor phosphorylation detected 1 min post Gas6 addition and maximal levels attained within 3 min (Fig. 6B and B'). Under these conditions, sustained high levels of Tyro3 phosphorylation were maintained for over 40 minutes. Gas6-induced Tyro3 phosphorylation was abrogated when Gas6 was preincubated with Tyro3-Fc receptor bodies for 30 min before addition to the cultured cells (Fig. 6C and C' compare lanes 2 and 3, top panel), demonstrating that Tyro3 receptor phosphorylation was a direct consequence of ligand addition.

Gas6 Activation of the MAPK Signaling Pathway in Cortical Neurons

As a first step toward identifying the downstream signaling pathways activated by Gas6 in cortical neurons, the ligand-dependent association of Tyro3 and the adaptor molecule Grb2 was assessed after activation with Gas6. This approach was based upon the presence of a predicted Grb2 SH2-domain consensus binding site in the Tyro3 sequence. A direct association of Grb2 with Tyro3 was induced upon Gas6 addition. This association was detected by Western blotting after immunoprecipitation of Tyro3 both in cortical (Fig. 7A, A' and A'') and hippocampal cells (not shown). Grb2 has been shown to induce activation of the ras/MAPkinase signaling pathway through its association with Sos; therefore the phosphorylation states of ERK1 and ERK2 were assessed using phosphospecific antibodies (Fig. 7B1 and B'1). The activation of ERK1/2 was also dependent on the concentration of Gas6. We then searched for possible targets activated by the Gas6-mediated induction of the ERKs. The RSK kinases are well-characterized downstream substrates for ERK1 and 2 in neurons (Xing et al., 1996, Thomas and Huganir, 2004). As shown in Fig. 7B, Gas6 induced the phosphorylation of RSK90 (Fig. 7B2 and B'2) and one of its targets, the transcription factor CREB (Fig. 7B3 and B'3), in a concentration dependent manner . A change in the phosphorylation of the transcription factor ELK-1, an ERK1/2 target, was not detected (not shown).

Gas6 Activation of the PI(3)K Signaling Pathway in Cortical Neurons

We then investigated the possibility that Gas6 could activate the PI(3)K pathway, a concept prompted by the presence of a consensus binding site for the p85 subunit of PI(3)K in the cytoplasmic tail of Tyro3. A previously reported yeast two-hybrid study implicated this site as a p85 binding partner (Lan et al., 2000). One of the major downstream targets for PI(3)K is the kinase AKT, whose activation can be detected using phospho-specific antibodies. As shown in Fig. 7C1 and C'1, activation by Gas6 increases the amount of phosphorylated AKT in a concentration dependent manner. A target of AKT in neurons and other cell types is the molecule mTOR, which has been shown to activate p70S6K (Cantley, 2002). As shown in Fig. 7C Gas6 increased the phosphorylation of both mTOR (Fig. 7C2 and C'2) and p70S6K (Fig. 7C3 and C'3). These results demonstrate that Gas6 can activate multiple components of both the PI(3)K and MAPK signaling pathways in cortical neurons. In dendrites, Gas6 signaling through Tyro3 is therefore well situated to modulate the neural activity-dependent stimulation of these pathways.

DISCUSSION

In the present study we examined the localization and signaling properties of the RPTK, Tyro3. This receptor is detected throughout the mature cortex and is also prominently expressed in the CA1 field of hippocampus. One of the most intriguing observations to emerge from this study was that the Tyro3 protein appeared as punctae distributed throughout the dendritic compartment of cortical and hippocampal neurons. The punctate pattern suggested that the

NIH-PA Author Manuscript

NIH-PA Author Manuscript

NIH-PA Author Manuscript

receptors were clustered and further prompted the question of whether these Tyro3 clusters may be localized to the synapse. The punctae were observed in both early (1 DIV) and later stage (8–20 DIV) cultures, implying that receptor clusters were present throughout neuronal development and at times prior to the formation of synapses. A number of dendritic proteins have been identified that exhibit a punctate pattern of expression. These include proteins enriched in the postsynaptic density such as PSD95, Shank, and the NMDA receptor subunit NR1 (Sheng and Kim, 2002). Tyro3 exhibited limited co-localization with PSD-95, suggesting that this receptor is primarily located outside of the postsynaptic density. In addition, Tyro3 did not appear to co-localize with GABA-A receptors (A.L.P. unpublished observations), which have been described as forming large clusters at synaptic sites and smaller clusters at extrasynaptic sites (Craig et al., 1994, Christie et al., 2002). Tyro3 also showed limited colocalization with the GABAergic presynaptic marker GAD-65 (Fig. 5C), which is preferentially localized to presynaptic GABAergic boutons (Benson et al., 1994). We have been unable to determine unequivocally whether Tyro3 is localized to the mature presynaptic terminal because the optimal staining conditions required for detecting this receptor are incompatible with those required to detect the presynaptic markers synaptophysin and synapsin. An ultrastructural analysis will be required to determine whether Tyro3 is present at presynaptic and postsynaptic sites. However, based on the limited co-localization with PSD-95 at the postsynaptic compartment and GAD-65 at presynaptic terminals, Tyro3 does not appear to be primarily localized to the synapse.

Several molecules have been identified that, like Tyro3, exhibit a punctate but largely non-synaptic distribution in dendrites *in vitro*. It is important to note that despite being located outside of the synapse, these molecules are capable of affecting signaling events initiated by neuronal synaptic activity. These include the signaling molecule p70S6K (Cammalleri et al., 2003) as well as components of the protein translation machinery important for activity-dependent protein synthesis (Sutton and Schuman, 2006) including the proteins staufen (Kiebler et al., 1999) and pumilio 2 (Vessey et al., 2006). In addition, clusters of the RPTK trkB have also been detected in the dendrites and axons of cortical neurons *in vitro* both before and after synapse formation. However, the localization of trkB differs from that of Tyro3 in that it becomes increasingly enriched at synapses as development proceeds. In non-synaptic sites trkB was detected in both stationary and mobile clusters, the latter being consistent with possible transport in synaptic vesicles (Gomes et al., 2006). These examples highlight the important issue that molecules localized or mobilized to the dendrites but located outside of the synapse have the ability to influence activity-dependent signaling.

Tyro3 was present not only in dendrites but also in growth cones as well as in the axonal compartment, suggesting a possible role for Tyro3 in axonal pathfinding. A role in cell adhesion and cell migration has been previously suggested for Axl (Bellosta et al., 1995). In addition, Gas6 signaling through Axl has been shown to promote the migration of vascular muscle endothelial cells (Fridell et al., 1998). At the structural level, TAM family members contain Ig-like domains and FN-type III repeats, motifs that are also present in molecules known to mediate cell-cell interactions such as the neural cell adhesion molecule N-CAM (Prieto and Crossin, 1995, Kamiguchi and Lemmon, 2000), members of the Robo receptor family that mediate the repulsive actions of the slit molecules on axons, and the deleted in colorectal cancer (DCC) receptor which mediates the attractive effects of netrins on axons (Chisholm and Tessier-Lavigne, 1999). These observations and the prominent presence of Tyro3 in the growth cone raise the possibility that Tyro3 may also play a role in axonal pathfinding.

In addition to being expressed in neurons, Tyro3 is also expressed in glial cells. In conjunction with our earlier efforts (Prieto et al., 2000), it is now evident that Tyro3 is expressed in radial glia, astrocytes and oligodendroglia. It appears that glia express more than one member of the TAM family since Axl is co-expressed with Tyro3 in Schwann cells where Gas6 induces cell

NIH-PA Author Manuscript

NIH-PA Author Manuscript

NIH-PA Author Manuscript

proliferation (Li et al., 1996). Axl was also detected in oligodendroglia (Prieto et al., 2000, Shankar et al., 2003). Axl has also been identified in microglia (Funakoshi et al., 2002) and in human malignant glioma cells (Vajkoczy et al., 2006). Mer has been detected in developing oligodendrocytes (Prieto et al., 2000) and in microglia (our unpublished observations). It will be important to determine the relative expression of each of the TAM receptors in these cell types as it has been reported that the levels of Tyro3 and Mer protein are co-regulated in retinal epithelial cells (Prasad et al., 2006).

Our previous studies have indicated that Gas6 mRNA and protein are expressed throughout the rat cortex and in most pyramidal cells in the hippocampus, as well as in a number of other regions in the CNS. In contrast, the expression of protein S mRNA was highly restricted with low levels of expression observed in the locus coeruleus and high levels in the choroid plexus (Prieto et al., 1999). In the rabbit brain, expression of protein S mRNA and protein has been reported in the cortex, hippocampal pyramidal neurons and granule neurons of the dentate gyrus (He et al., 1995). Protein S has also been detected in cells of the glial lineage *in vitro*, including several glioblastomas and one neuroblastoma cell line (Phillips et al., 1993). Given the increased interest in the role of protein S as a TAM family ligand, it would be important to address these apparent discrepancies by evaluating the expression profiles of protein S and Gas6 in additional species, and by further exploring how the postranslational modifications of these gene products may influence their signaling abilities.

The presence of Tyro3 in dendrites, a compartment critical for integrating synaptic inputs, suggests that it may initiate signaling events capable of modulating activity-dependent neuronal plasticity. In support of this hypothesis, it has been reported that young adult Tyro3 knockout mice exhibit a decrease in LTP (Lemke and Lu, 2003). Our findings have revealed that Gas6 stimulation of Tyro3 is capable of activating several components of the MAPK and PI(3)K signaling pathways, both of which play key roles in the molecular events underlying neuronal plasticity (Thomas and Huganir, 2004). Therefore, the other major finding of this study is that Tyro3 may serve as a heretofore unrecognized modulator of MAPK and PI(3)K signaling in neuronal dendrites.

We have demonstrated that Gas6 can activate the MAPK pathway through the phosphorylation of two MAP kinases, ERK 1 and 2 (see Figs. 7B). Gas6 has been previously shown to induce ERK1/2 phosphorylation in mature mouse osteoclasts (Katagiri et al., 2001). One possible mechanism of MAPK/Erk1/2 activation is by the direct or indirect recruitment of Grb2 by RPTKs (Kouhara et al., 1997). Our data have indicated that Grb2 can directly interact with Tyro3 (Fig. 7A), providing one avenue for the activation of the MAPK pathway. In neurons, activation of the MAPK signaling pathways through Grb2 has been reported for several members of the Eph (Pasquale, 2005) and trk RPTK families (Reichardt, 2006).

What are the possible targets of Gas6-induced ERK1/2 activation? Two candidates have been identified in this study, RSK and CREB. RSK has been previously shown to regulate CREB phosphorylation at ser133 in response to growth factors such as EGF and the neurotrophins (Ginty et al., 1994), and we have observed that Gas6 activation also leads to phosphorylation on this residue. CREB and its coactivators have been shown to function as molecular regulators of gene expression leading to the transcriptional regulation of a large set of genes (West et al., 2001) implicated in the alteration of complex processes such as the consolidation of memories, addictive behaviors, and circadian rhythms (Lonze and Ginty, 2002). Additional studies will be required to determine the functional consequences of ser133CREB phosphorylation in response to Gas6.

Our studies have also demonstrated that Gas6 activates multiple components the PI(3)K pathway in neurons. Tyro3 bears a single consensus binding site for the p85 regulatory subunit

NIH-PA Author Manuscript

NIH-PA Author Manuscript

NIH-PA Author Manuscript

of PI(3)K. Although we have been able to detect a direct association between Tyro3 and p85 in a fibroblastic cell line overexpressing p85 (not shown), we have been unable to demonstrate a direct association in neurons. Thus the precise mechanism of the Gas6-mediated PI(3)K activation in neurons is not understood and it is conceivable that the PI(3)K signaling pathway is being activated indirectly, possibly through ras (Cantley, 2002).

We have also detected Gas6/Tyro3 mediated activation of three other members of the PI(3)K signaling pathway, AKT, which along with PDK1 serves as one of the main targets of PI(3)K (Cantley, 2002), mTOR and p70S6K which can act downstream of AKT. What are the potential consequences in cortical neurons of Tyro3 activation of these molecules? One possibility, although speculative, is that Tyro3 activation can regulate protein translation, since activated mTOR can phosphorylate and activate p70S6K, which in turn phosphorylates the S6 ribosomal protein (Shaw and Cantley, 2006). mTOR can also phosphorylate inhibitors of translation such as 4E-BP1, resulting in enhanced translation.

In neurons, the PI(3)K pathway has also been implicated as a modulator of synaptic plasticity (Sweatt, 2001, Opazo et al., 2003). Activity-dependent protein translation is mediated by p70S6K in the dendritic compartment even though this kinase is primarily found in the dendritic shaft and to a lesser extent in the dendritic spines (Aakalu et al., 2001, Cammalleri et al., 2003). It should be noted that ERK1/2 activated by Gas6/Tyro3 could also induce mTOR activation. The relative contribution of the MAPK and AKT pathways to the Gas6-mediated activation of mTOR remains to be established. The ability of Gas6 to stimulate the phosphorylation of AKT/mTOR/p70S6kinase suggests a potential role for Tyro3 as a regulator of translation in dendrites.

In summary, our studies have revealed that Tyro3 is a receptor protein tyrosine kinase expressed in dendrites that is capable of activating signaling pathways known to modulate synaptic plasticity. These findings suggest that Gas6 activation of Tyro3 may influence synaptic transmission.

Acknowledgements

We acknowledge the help provided by Dr. Barry Stein from the Molecular Biology Institute at IU Bloomington with the fluorescent microscopy. We also thank Greg Lemke from the Salk Institute for providing the Rat2/Tyro3 transfected cells. We wish to thank Dr. Michael Walker and Harini Hughes for critical reading of the manuscript and Dr. Olaf Sporns for help with the data analysis. We also wish to thank Dr. Cara Wellman for the use of her microscope, and Dr. James Drummond for the use of his imaging system. This work was supported in part by the NIH (NS37471 to ALP and NS32367 to CL) and the National Science Foundation (NSF0136383 to ALP). This research was also supported by an Indiana University FRSP award to ALP and by the Indiana METACyt Initiative of Indiana University, funded through a major grant from the Lilly Endowment, Inc, Indianapolis IN.

References

Aakalu G, Smith WB, Nguyen N, Jiang C, Schuman EM. Dynamic visualization of local protein synthesis in hippocampal neurons. Neuron 2001;30:489–502. [PubMed: 11395009]

Allen MP, Zeng C, Schneider K, Xiong X, Meintzer MK, Bellosta P, Basilico C, Varnum B, Heidenreich KA, Wierman ME. Growth arrest-specific gene 6 (Gas6)/adhesion related kinase (Ark) signaling promotes gonadotropin-releasing hormone neuronal survival via extracellular signal-regulated kinase (ERK) and Akt. Molecular endocrinology (Baltimore, Md) 1999;13:191–201.

Angelillo-Scherrer A, Burnier L, Flores N, Savi P, DeMol M, Schaeffer P, Herbert JM, Lemke G, Goff SP, Matsushima GK, Earp HS, Vesin C, Hoylaerts MF, Plaisance S, Collen D, Conway EM, Wehrle-Haller B, Carmeliet P. Role of Gas6 receptors in platelet signaling during thrombus stabilization and implications for antithrombotic therapy. J Clin Invest 2005;115:237–246. [PubMed: 15650770]

Arthur JS, Fong AL, Dwyer JM, Davare M, Reese E, Obrietan K, Impey S. Mitogen- and stress-activated protein kinase 1 mediates cAMP response element-binding protein phosphorylation and activation by neurotrophins. J Neurosci 2004;24:4324–4332. [PubMed: 15128846]

NIH-PA Author Manuscript

NIH-PA Author Manuscript

NIH-PA Author Manuscript

Banker Ga, GK. Culturing Nerve Cells Cambridge. Massachusetts: MIT Press; 2002.

Bellosta P, Costa M, Lin DA, Basilico C. The receptor tyrosine kinase ARK mediates cell aggregation by homophilic binding. Mol Cell Biol 1995;15:614–625. [PubMed: 7823930]

Benson DL, Watkins FH, Steward O, Banker G. Characterization of GABAergic neurons in hippocampal cell cultures. J Neurocytol 1994;23:279–295. [PubMed: 8089704]

Blum R, Konnerth A. Neurotrophin-mediated rapid signaling in the central nervous system: mechanisms and functions. Physiology (Bethesda, Md) 2005;20:70–78.

Brewer GJ, Torricelli JR, Evege EK, Price PJ. Optimized survival of hippocampal neurons in B27-supplemented Neurobasal, a new serum-free medium combination. J Neurosci Res 1993;35:567–576. [PubMed: 8377226]

Cammalleri M, Lutjens R, Berton F, King AR, Simpson C, Francesconi W, Sanna PP. Time-restricted role for dendritic activation of the mTOR-p70S6K pathway in the induction of late-phase long-term potentiation in the CA1. Proc Natl Acad Sci U S A 2003;100:14368–14373. [PubMed: 14623952]

Cantley LC. The phosphoinositide 3-kinase pathway. Science 2002;296:1655–1657. [PubMed: 12040186]

Caraux A, Lu Q, Fernandez N, Riou S, Di Santo JP, Raulet DH, Lemke G, Roth C. Natural killer cell differentiation driven by Tyro3 receptor tyrosine kinases. Nature immunology 2006;7:747–754. [PubMed: 16751775]

Chisholm A, Tessier-Lavigne M. Conservation and divergence of axon guidance mechanisms. Curr Opin Neurobiol 1999;9:603–615. [PubMed: 10508749]

Christie SB, Miralles CP, De Blas AL. GABAergic innervation organizes synaptic and extrasynaptic GABAA receptor clustering in cultured hippocampal neurons. J Neurosci 2002;22:684–697. [PubMed: 11826098]

Craig AM, Blackstone CD, Huganir RL, Banker G. Selective clustering of glutamate and gamma-aminobutyric acid receptors opposite terminals releasing the corresponding neurotransmitters. Proc Natl Acad Sci U S A 1994;91:12373–12377. [PubMed: 7809044]

D'Cruz PM, Yasumura D, Weir J, Matthes MT, Abderrahim H, LaVail MM, Vollrath D. Mutation of the receptor tyrosine kinase gene Mertk in the retinal dystrophic RCS rat. Human molecular genetics 2000;9:645–651. [PubMed: 10699188]

Fridell YW, Villa J Jr, Attar EC, Liu ET. GAS6 induces Axl-mediated chemotaxis of vascular smooth muscle cells. J Biol Chem 1998;273:7123–7126. [PubMed: 9507025]

Funakoshi H, Yonemasu T, Nakano T, Matumoto K, Nakamura T. Identification of Gas6, a putative ligand for Sky and Axl receptor tyrosine kinases, as a novel neurotrophic factor for hippocampal neurons. J Neurosci Res 2002;68:150–160. [PubMed: 11948660]

Ginty DD, Bonni A, Greenberg ME. Nerve growth factor activates a Ras-dependent protein kinase that stimulates c-fos transcription via phosphorylation of CREB. Cell 1994;77:713–725. [PubMed: 8205620]

Godowski PJ, Mark MR, Chen J, Sadick MD, Raab H, Hammonds RG. Reevaluation of the roles of protein S and Gas6 as ligands for the receptor tyrosine kinase Rse/Tyro 3. Cell 1995;82:355–358. [PubMed: 7634325]

Gomes RA, Hampton C, El-Sabeawy F, Sabo SL, McAllister AK. The dynamic distribution of TrkB receptors before, during, and after synapse formation between cortical neurons. J Neurosci 2006;26:11487–11500. [PubMed: 17079678]

Hafizi S, Dahlback B. Gas6 and protein S. The FEBS journal 2006a;273:5231–5244. [PubMed: 17064312]

Hafizi S, Dahlback B. Signalling and functional diversity within the Axl subfamily of receptor tyrosine kinases. Cytokine & growth factor reviews 2006b;17:295–304. [PubMed: 16737840]

Hafizi S, Gustafsson A, Stenhoff J, Dahlback B. The Ran binding protein RanBPM interacts with Axl and Sky receptor tyrosine kinases. The international journal of biochemistry & cell biology 2005;37:2344–2356.

Hall MO, Obin MS, Heeb MJ, Burgess BL, Abrams TA. Both protein S and Gas6 stimulate outer segment phagocytosis by cultured rat retinal pigment epithelial cells. Experimental eye research 2005;81:581–591. [PubMed: 15949798]

NIH-PA Author Manuscript

NIH-PA Author Manuscript

NIH-PA Author Manuscript

He X, Shen L, Bjartell A, Dahlback B. The gene encoding vitamin K-dependent anticoagulant protein S is expressed in multiple rabbit organs as demonstrated by northern blotting, in situ hybridization, and immunohistochemistry. J Histochem Cytochem 1995;43:85–96. [PubMed: 7822769]

Hipskind RA, Rao VN, Mueller CG, Reddy ES, Nordheim A. Ets-related protein Elk-1 is homologous to the c-fos regulatory factor p62TCF. Nature 1991;354:531–534. [PubMed: 1722028]

Huang YZ, Won S, Ali DW, Wang Q, Tanowitz M, Du QS, Pelkey KA, Yang DJ, Xiong WC, Salter MW, Mei L. Regulation of neuregulin signaling by PSD-95 interacting with ErbB4 at CNS synapses. Neuron 2000;26:443–455. [PubMed: 10839362]

Kamiguchi H, Lemmon V. IgCAMs: bidirectional signals underlying neurite growth. Curr Opin Cell Biol 2000;12:598–605. [PubMed: 10978896]

Katagiri M, Hakeda Y, Chikazu D, Ogasawara T, Takato T, Kumegawa M, Nakamura K, Kawaguchi H. Mechanism of stimulation of osteoclastic bone resorption through Gas6/Tyro 3, a receptor tyrosine kinase signaling, in mouse osteoclasts. J Biol Chem 2001;276:7376–7382. [PubMed: 11084030]

Kiebler MA, Hemraj I, Verkade P, Kohrmann M, Fortes P, Marion RM, Ortin J, Dotti CG. The mammalian staufen protein localizes to the somatodendritic domain of cultured hippocampal neurons: implications for its involvement in mRNA transport. J Neurosci 1999;19:288–297. [PubMed: 9870958]

Kouhara H, Hadari YR, Spivak-Kroizman T, Schilling J, Bar-Sagi D, Lax I, Schlessinger J. A lipid-anchored Grb2-binding protein that links FGF-receptor activation to the Ras/MAPK signaling pathway. Cell 1997;89:693–702. [PubMed: 9182757]

Kwon OB, Longart M, Vullhorst D, Hoffman DA, Buonanno A. Neuregulin-1 reverses long-term potentiation at CA1 hippocampal synapses. J Neurosci 2005;25:9378–9383. [PubMed: 16221846]

Lai C, Gore M, Lemke G. Structure, expression, and activity of Tyro 3, a neural adhesion-related receptor tyrosine kinase. Oncogene 1994;9:2567–2578. [PubMed: 8058320]

Lan Z, Wu H, Li W, Wu S, Lu L, Xu M, Dai W. Transforming activity of receptor tyrosine kinase tyro3 is mediated, at least in part, by the PI3 kinase-signaling pathway. Blood 2000;95:633–638. [PubMed: 10627473]

Lein ES, Zhao X, Gage FH. Defining a molecular atlas of the hippocampus using DNA microarrays and high-throughput in situ hybridization. J Neurosci 2004;24:3879–3889. [PubMed: 15084669]

Lemke G, Lu Q. Macrophage regulation by Tyro 3 family receptors. Current opinion in immunology 2003;15:31–36. [PubMed: 12495730]

Li R, Chen J, Hammonds G, Phillips H, Armanini M, Wood P, Bunge R, Godowski PJ, Sliwkowski MX, Mather JP. Identification of Gas6 as a growth factor for human Schwann cells. J Neurosci 1996;16:2012–2019. [PubMed: 8604045]

Lonze BE, Ginty DD. Function and regulation of CREB family transcription factors in the nervous system. Neuron 2002;35:605–623. [PubMed: 12194863]

Lu Q, Gore M, Zhang Q, Camenisch T, Boast S, Casagranda F, Lai C, Skinner MK, Klein R, Matsushima GK, Earp HS, Goff SP, Lemke G. Tyro-3 family receptors are essential regulators of mammalian spermatogenesis. Nature 1999;398:723–728. [PubMed: 10227296]

Malenka RC, Nicoll RA. Long-term potentiation--a decade of progress? Science 1999;285:1870–1874. [PubMed: 10489359]

Manfioletti G, Brancolini C, Avanzi G, Schneider C. The protein encoded by a growth arrest-specific gene (gas6) is a new member of the vitamin K-dependent proteins related to protein S, a negative coregulator in the blood coagulation cascade. Mol Cell Biol 1993;13:4976–4985. [PubMed: 8336730]

Mark MR, Chen J, Hammonds RG, Sadick M, Godowsk PJ. Characterization of Gas6, a member of the superfamily of G domain-containing proteins, as a ligand for Rse and Axl. J Biol Chem 1996;271:9785–9789. [PubMed: 8621659]

Nagata K, Ohashi K, Nakano T, Arita H, Zong C, Hanafusa H, Mizuno K. Identification of the product of growth arrest-specific gene 6 as a common ligand for Axl, Sky, and Mer receptor tyrosine kinases. J Biol Chem 1996;271:30022–30027. [PubMed: 8939948]

Nyberg P, He X, Hardig Y, Dahlback B, Garcia de Frutos P. Stimulation of Sky tyrosine phosphorylation by bovine protein S--domains involved in the receptor-ligand interaction. European journal of biochemistry/FEBS 1997;246:147–154. [PubMed: 9210477]

NIH-PA Author Manuscript

NIH-PA Author Manuscript

NIH-PA Author Manuscript

Opazo P, Watabe AM, Grant SG, O'Dell TJ. Phosphatidylinositol 3-kinase regulates the induction of long-term potentiation through extracellular signal-related kinase-independent mechanisms. J Neurosci 2003;23:3679–3688. [PubMed: 12736339]

Pasquale EB. Eph receptor signalling casts a wide net on cell behaviour. Nat Rev Mol Cell Biol 2005;6:462–475. [PubMed: 15928710]

Pearson G, Robinson F, Beers Gibson T, Xu BE, Karandikar M, Berman K, Cobb MH. Mitogen-activated protein (MAP) kinase pathways: regulation and physiological functions. Endocrine reviews 2001;22:153–183. [PubMed: 11294822]

Phillips DJ, Greengard JS, Fernandez JA, Ribeiro M, Evatt BL, Griffin JH, Hooper WC. Protein S, an antithrombotic factor, is synthesized and released by neural tumor cells. J Neurochem 1993;61:344–347. [PubMed: 8515282]

Prasad D, Rothlin CV, Burrola P, Burstyn-Cohen T, Lu Q, Garcia de Frutos P, Lemke G. TAM receptor function in the retinal pigment epithelium. Mol Cell Neurosci 2006;33:96–108. [PubMed: 16901715]

Prieto AL, Crossin KL. Cell-cell adhesion molecules in epithelial-mesenchymal transformations. Acta anatomica 1995;154:21–33. [PubMed: 8714287]

Prieto AL, Weber JL, Lai C. Expression of the receptor protein-tyrosine kinases Tyro-3, Axl, and mer in the developing rat central nervous system. J Comp Neurol 2000;425:295–314. [PubMed: 10954847]

Prieto AL, Weber JL, Tracy S, Heeb MJ, Lai C. Gas6, a ligand for the receptor protein-tyrosine kinase Tyro-3, is widely expressed in the central nervous system. Brain Res 1999;816:646–661. [PubMed: 9878891]

Reichardt LF. Neurotrophin-regulated signalling pathways. Philosophical transactions of the Royal Society of London 2006;361:1545–1564. [PubMed: 16939974]

Schlessinger J. Cell signaling by receptor tyrosine kinases. Cell 2000;103:211–225. [PubMed: 11057895]

Shankar SL, O'Guin K, Cammer M, McMorris FA, Stitt TN, Basch RS, Varnum B, Shafit-Zagardo B. The growth arrest-specific gene product Gas6 promotes the survival of human oligodendrocytes via a phosphatidylinositol 3-kinase-dependent pathway. J Neurosci 2003;23:4208–4218. [PubMed: 12764109]

Shankar SL, O'Guin K, Kim M, Varnum B, Lemke G, Brosnan CF, Shafit-Zagardo B. Gas6/Axl signaling activates the phosphatidylinositol 3-kinase/Akt1 survival pathway to protect oligodendrocytes from tumor necrosis factor alpha-induced apoptosis. J Neurosci 2006;26:5638–5648. [PubMed: 16723520]

Shaw RJ, Cantley LC. Ras, PI(3)K and mTOR signalling controls tumour cell growth. Nature 2006;441:424–430. [PubMed: 16724053]

Sheng M, Kim MJ. Postsynaptic signaling and plasticity mechanisms. Science 2002;298:776–780. [PubMed: 12399578]

Songyang Z, Shoelson SE, Chaudhuri M, Gish G, Pawson T, Haser WG, King F, Roberts T, Ratnofsky S, Lechleider RJ, et al. SH2 domains recognize specific phosphopeptide sequences. Cell 1993;72:767–778. [PubMed: 7680959]

Stitt TN, Conn G, Gore M, Lai C, Bruno J, Radziejewski C, Mattsson K, Fisher J, Gies DR, Jones PF, et al. The anticoagulation factor protein S and its relative, Gas6, are ligands for the Tyro 3/Axl family of receptor tyrosine kinases. Cell 1995;80:661–670. [PubMed: 7867073]

Sutton MA, Schuman EM. Dendritic protein synthesis, synaptic plasticity, and memory. Cell 2006;127:49–58. [PubMed: 17018276]

Sweatt JD. Protooncogenes subserve memory formation in the adult CNS. Neuron 2001;31:671–674. [PubMed: 11567607]

Thomas GM, Huganir RL. MAPK cascade signalling and synaptic plasticity. Nature reviews 2004;5:173–183.

Toshima J, Ohashi K, Iwashita S, Mizuno K. Autophosphorylation activity and association with Src family kinase of Sky receptor tyrosine kinase. Biochem Biophys Res Commun 1995;209:656–663. [PubMed: 7537495]

Vajkoczy P, Knyazev P, Kunkel A, Capelle HH, Behrndt S, von Tengg-Kobligk H, Kiessling F, Eichelsbacher U, Essig M, Read TA, Erber R, Ullrich A. Dominant-negative inhibition of the Axl receptor tyrosine kinase suppresses brain tumor cell growth and invasion and prolongs survival. Proc Natl Acad Sci U S A 2006;103:5799–5804. [PubMed: 16585512]

NIH-PA Author Manuscript

NIH-PA Author Manuscript

NIH-PA Author Manuscript

Varnum BC, Young C, Elliott G, Garcia A, Bartley TD, Fridell YW, Hunt RW, Trail G, Clogston C, Toso RJ, et al. Axl receptor tyrosine kinase stimulated by the vitamin K-dependent protein encoded by growth-arrest-specific gene 6. Nature 1995;373:623–626. [PubMed: 7854420]

Vessey JP, Vaccani A, Xie Y, Dahm R, Karra D, Kiebler MA, Macchi P. Dendritic localization of the translational repressor Pumilio 2 and its contribution to dendritic stress granules. J Neurosci 2006;26:6496–6508. [PubMed: 16775137]

West AE, Chen WG, Dalva MB, Dolmetsch RE, Kornhauser JM, Shaywitz AJ, Takasu MA, Tao X, Greenberg ME. Calcium regulation of neuronal gene expression. Proc Natl Acad Sci U S A 2001;98:11024–11031. [PubMed: 11572963]

Xing J, Ginty DD, Greenberg ME. Coupling of the RAS-MAPK pathway to gene activation by RSK2, a growth factor-regulated CREB kinase. Science 1996;273:959–963. [PubMed: 8688081]

List of Abbreviations

Ax
: axon

BDNF
: brain derived neurotrophic factor

BSA
: bovine serum albumin

CNPase
: 2', 3' cyclic nucleotide 3'-phosphodiesterase

CNS
: central nervous system

DAB
: diaminobenzidine

DAPI
: 4’, 6-diamidino-2-phenylindole dihydrochloride

DIV
: days *in vitro*

DMEM
: Dulbecco Modified Eagle's Minimal Essential Medium

FCS
: fetal calf serum

FN
: fibronectin

E
: embryonic

EGF
: epidermal growth factor

ERK
: extracellular signal-regulated protein kinase

HBSS
: Hank’s balanced salt solution

NIH-PA Author Manuscript

NIH-PA Author Manuscript

NIH-PA Author Manuscript

HRP
horse radish peroxidase

Ig
immunoglobulin

IP
immunoprecipitation

GABA
γ-aminobutyric acid

GAD
glutamic acid decarboxylase

Gas6
growth arrest-specific gene6

Gc
growth cone

GFAP
glial fibrilliary acidic protein

Gla
γ-carboxylated glutamic acid

GPI
glycosylphosphatidylinositol

GST
glutathione -S-transferase

LTP
long-term potentiation

MAP-2
microtubule-associated protein 2

MAPK
mitogen-activated protein kinase

MSK
mitogen- and stress–activated protein kinase

mTOR
mammalian target of rapamycin

P
postnatal

p
phospho

ptyr
phosphotyrosine

PB
phosphate buffer

NIH-PA Author Manuscript

NIH-PA Author Manuscript

NIH-PA Author Manuscript

PBS
phosphate-buffered saline

PCR
polymerase chain reaction

PI(3)K
phosphoinositide-3 kinase

TAM
Tyro3, Axl, and Mer

TBS
Tris-buffered saline

TNF
tumor necrosis factor

RPTKs
receptor protein tyrosine kinases

RSK
ribosomal protein S6 kinase

SDS-PAGE
sodium dodecylsulphate polyacrylamide gel electrophoresis

SHBG
steroid hormone-binding protein

NIH-PA Author Manuscript
NIH-PA Author Manuscript
NIH-PA Author Manuscript

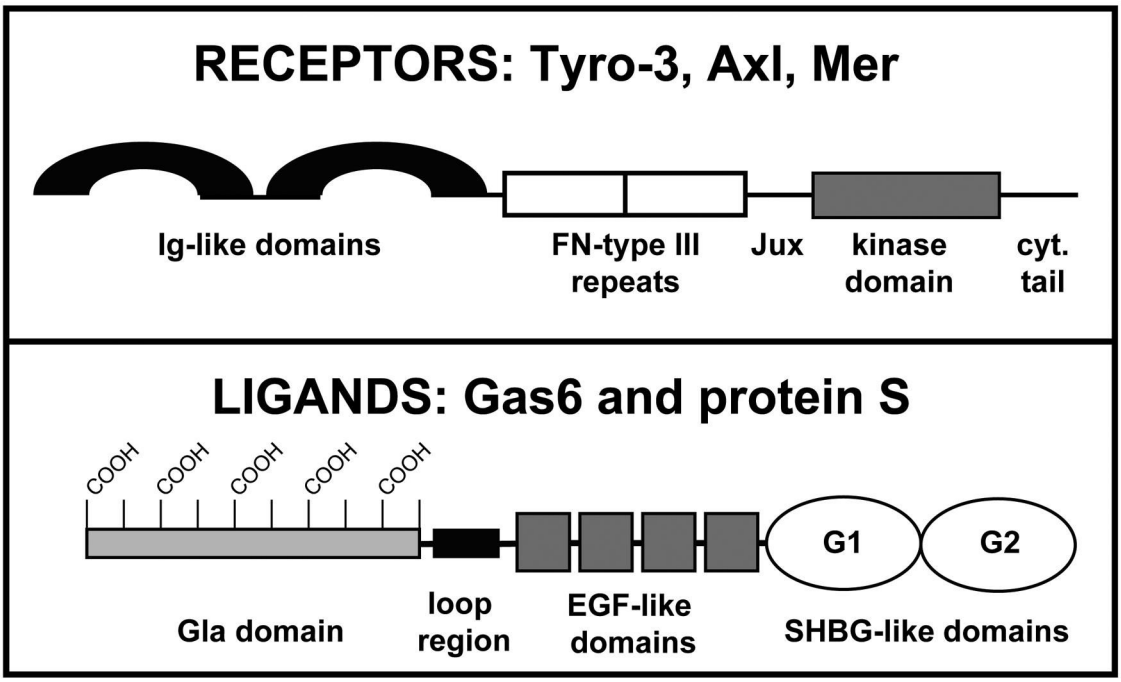

Figure 1. Model of the domain structure of the TAM receptor family and its ligands Gas6 and protein S

(Top) Model of the structure of the TAMs (Tyro3, Axl, and Mer). Extracellular domain: 2 Immunoglobulin (Ig)-like domains and 2 fibronectin (FN)-type III repeats. Intracellular domain: juxtamembrane region (Jux), a conserved kinase domain and the cytoplasmic tail (Cyt.Tail) (Lai et al., 1994). **(Bottom)** Model of the structure of the Gas6 (growth arrest-specific gene 6) and protein S. Gla domain for γ-carboxylated domain, the loop region, 4 epidermal growth factor (EGF)-like domains and the steroid hormone-binding like domain (SHBG) (Manfioletti et al., 1993). The SHBG domain is constituted of 2 globular domains initially identified in laminin (G1 and G2) (Manfioletti et al., 1993).

NIH-PA Author Manuscript

NIH-PA Author Manuscript

NIH-PA Author Manuscript

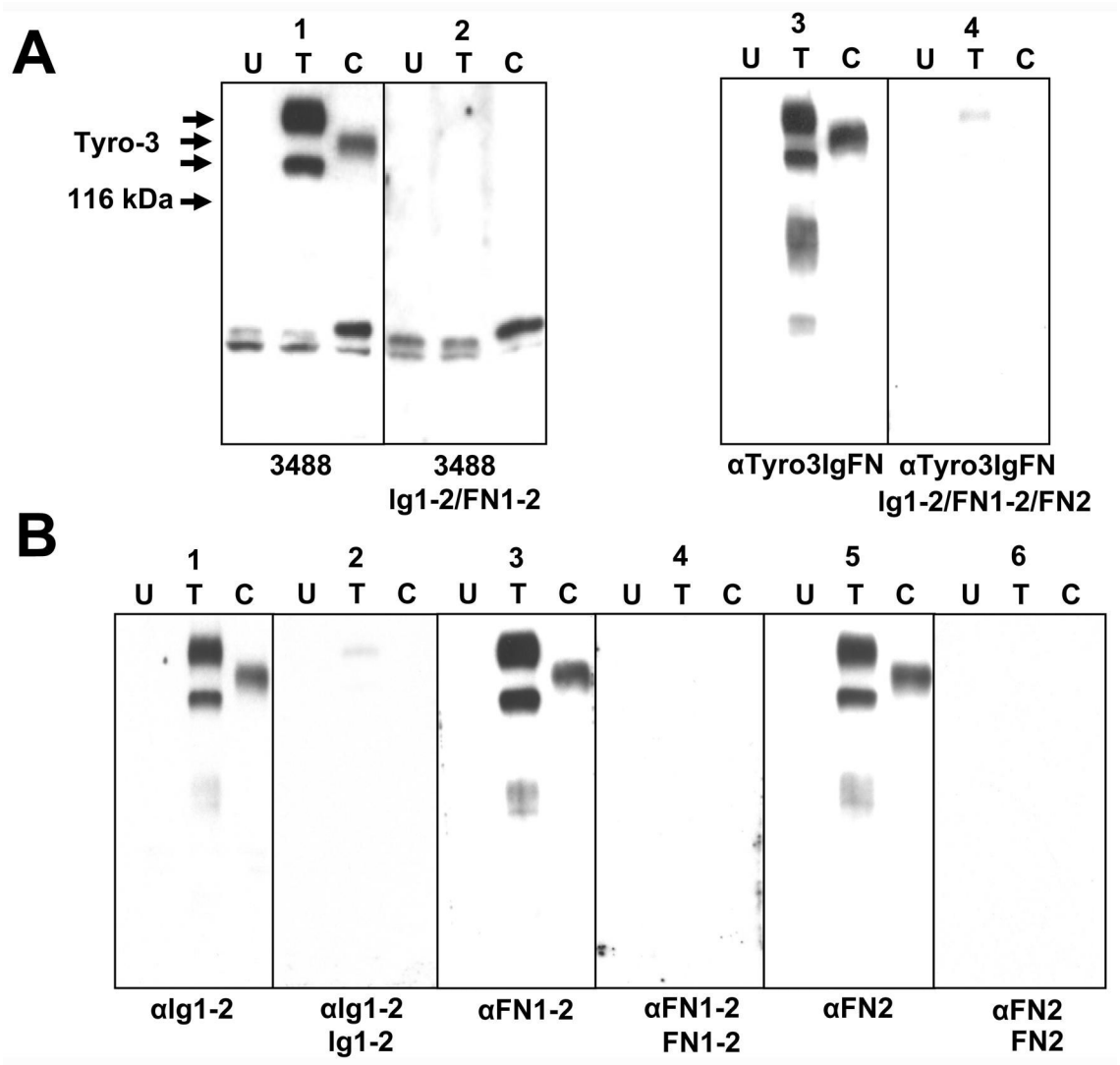

Figure 2. Characterization of extracellular domain-specific Tyro3 antibodies

Antibodies were tested for their ability to recognize Tyro3 by Western blot analysis **(A and B)**. For Western blotting, detergent extracts corresponding to 50 μg of protein per lane of Rat2 control **(lane U)**, Rat2/Tyro3 transfected cell extracts **(lane T),** or cortical brain extracts **(lane C)** were used to detect Tyro3. The blots were probed with: **Top Panels; panel 1A**, serum #3488, **panel 2A** serum #3488 preabsorbed with a mixture of Ig1-2GST and FN1-2GST; **panel 3A**, a mixture of 3 affinity purified antibodies (anti-Tyro3IgFN mix) consisting of affinity purified anti-Ig1-2, anti-FN1-2 and anti-FN2; **panel 4A**, anti-Tyro3IgFN mix preabsorbed with a mixture of Ig1-2GST, FN1-2GST and FN2GST. **Bottom panels: panel 1B,** affinity purified anti-Ig1-2; **panel 2B**, affinity purified anti-Ig1-2 preabsorbed with Ig1-2GST; **panel 3B**, affinity purified anti-FN1-2; **panel 4B**, affinity purified anti-FN1-2 preabsorbed with FN1-2GST; **panel 5B**, affinity purified anti-FN2; **panel 6B**, affinity purified anti-FN2 preabsorbed with FN2GST.

NIH-PA Author Manuscript
NIH-PA Author Manuscript
NIH-PA Author Manuscript

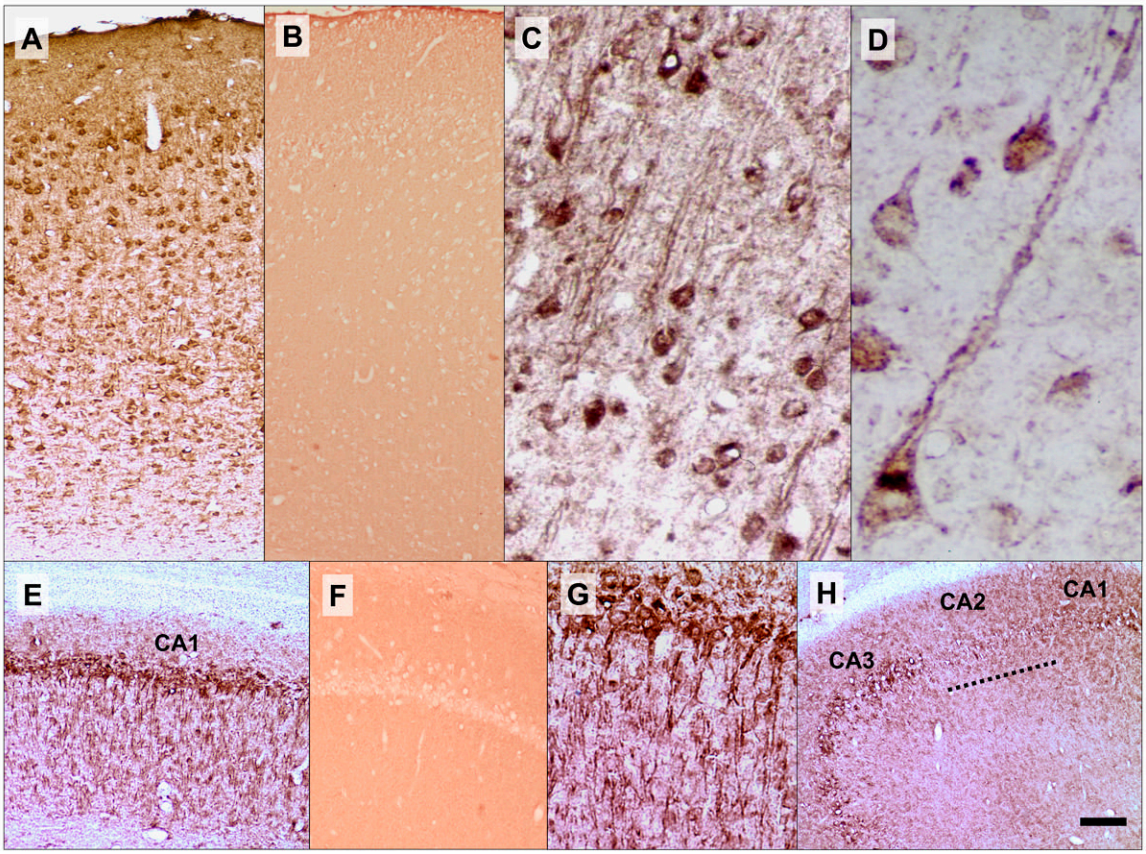

Figure 3. Tyro3 expression in the rat cerebral cortex and the hippocampus

Coronal sections (10 μm) of P52 rat brains were stained with anti-Tyro3 serum #3488 (1:200) (panels **A, C, D, E, G** and **H**) or serum #3488 preabsorbed with Ig1-2GST and FN1-2GST (panels **B** and **F**). Antibody immunoreactivity in adult rat cortex and hippocampus was visualized with biotinylated goat anti-rabbit antibodies (1:200) followed by biotin-avidin incubation and diaminobenzidine (DAB) staining **(A-H)**. Tyro3 is expressed in the majority of cells throughout all layers of the cortex **(A).** Higher magnification images show Tyro3 expression in dendrites of pyramidal neurons **(C** and **D)** with prominent staining on the cell surface as evidenced by the hollow aspect of the dendritic shafts. The cell bodies and the dendrites of CA1 pyramidal neurons are clearly labeled for Tyro3 **(E and G)** while CA2 neurons do not appear to express detectable levels of this protein **(H).** Staining using serum #3488 preabsorbed with the Tyro3 antigens showed no significant staining in either the cortex (**B**) or hippocampus (**F**). Scale bar= 130 μm for **A** and **B**, 20 μm for **C,** 10μm for **D**, 280 μm for **E** and **F**, 85 μm for **G**, and 160 μm for **H**.

NIH-PA Author Manuscript
NIH-PA Author Manuscript
NIH-PA Author Manuscript

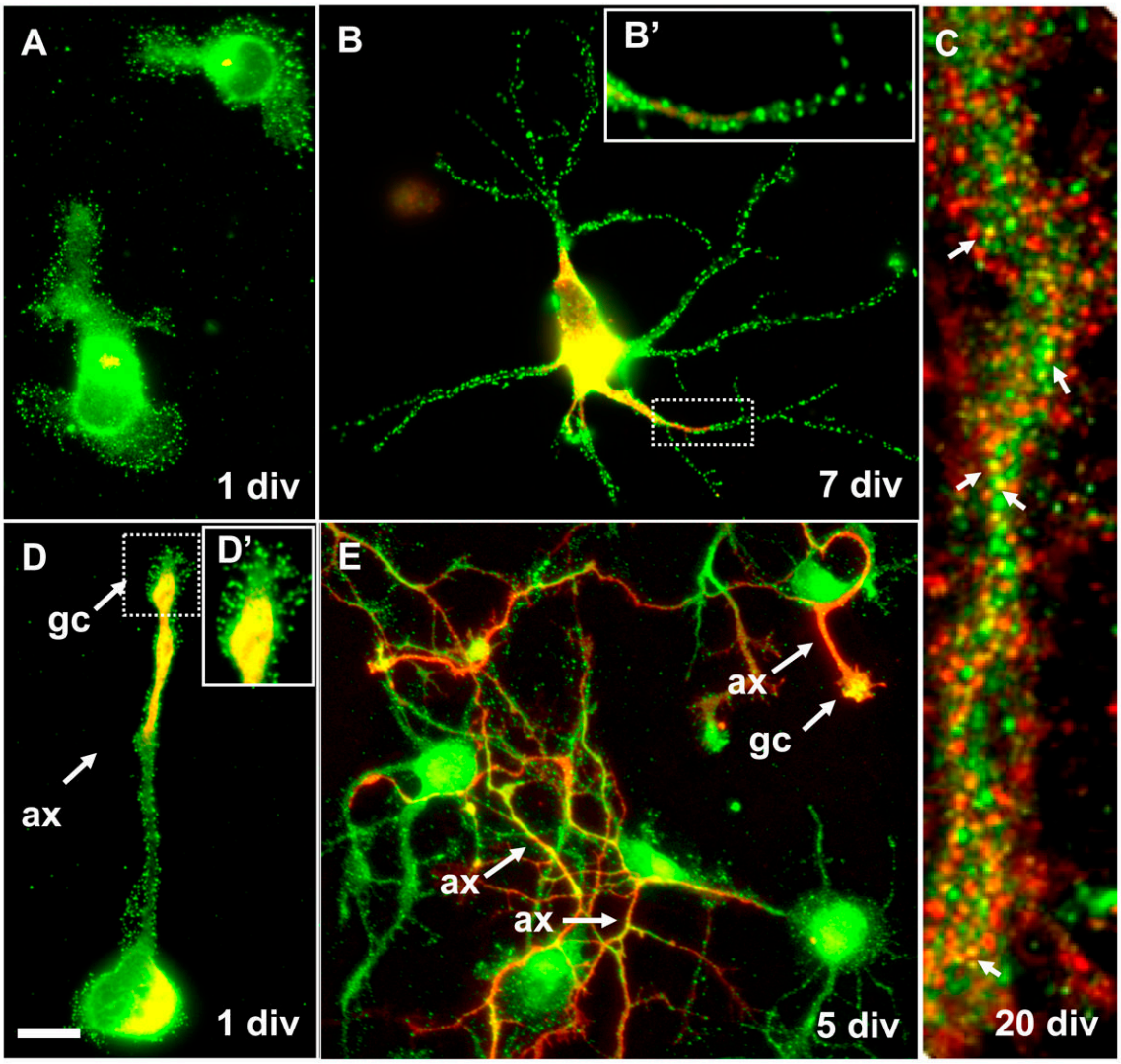

Figure 4. Punctate expression of Tyro3 in dendrites and axons of dissociated hippocampal neurons

Immunofluorescent staining of primary hippocampal cultures of 1 day *in vitro* (div) (panels **A, D,** and **D'**), 7 div (**B** and **B'**), 5 div (**E**), and 20 div (**C**). The cell cultures were double labeled as follows: panel **A**, anti-Tyro3IgFN and anti-synaptophysin; **panels B** and **B'**, anti-Tyro3IgFN and anti-actin antibodies; panel **C**, anti-Tyro3IgFN and anti-PSD-95 antibodies; panels **D**, **D'** and **E,** anti-Tyro3IgFN and anti-tau antibodies. Panels**, B'** and **D'** are enlarged views of the boxed areas in **B** and **D** respectively. Tyro3 does not extensively colocalize with the postsynaptic PSD-95 marker (panel **C**). Arrows identify a few punctae where the molecules are colocalized. The staining shown in panels **A, B** and **D** was done in the absence of detergent. This resulted in only partial penetration of the antibodies against cytoplasmic proteins but preserved the punctate Tyro3 staining. The staining shown in panels **C** and **E** was performed in the presence of 0.1% Triton-X 100. Anti-synaptophysin, anti-actin, anti-PSD-95 and anti-tau antibodies were labeled with secondary antibodies coupled with Alexa Fluor 594 in red, and anti-Tyro3 antibodies were labeled with secondary antibodies coupled to AlexaFluor 488 in green. Ax, axon, gc, growth cone. Scale bar= 30 μm for **A**, 30 μm for **B**, 10 μm for **B'**, 5 μm for **C**, 25 μm for **D,** 15 μm for **D',** 40 μm for **E**.

NIH-PA Author Manuscript
NIH-PA Author Manuscript
NIH-PA Author Manuscript

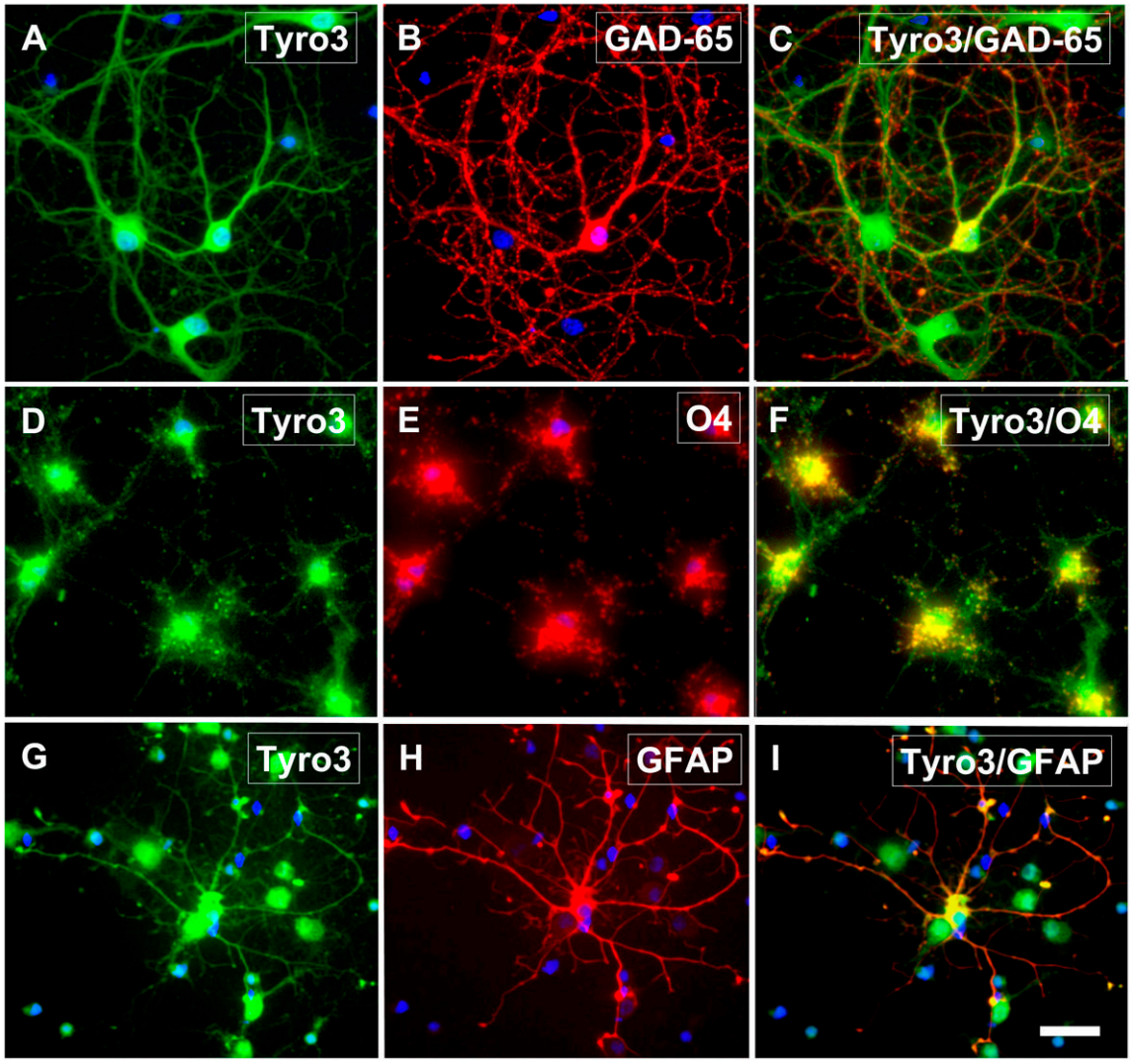

Figure 5. Tyro3 is expressed in GABAergic neurons and glial cells

Cultures of cortical cells (14 days *in vitro)* were double-stained with anti-Tyro3IgFN antibodies (panels **A**, **D and G**), with anti-GAD-65 antibodies to label GABAergic neurons (panels **B and C),** with anti-O4 to label oligodendrocyte precursors (panels **E** and **F**) and with anti-GFAP antibodies to label astrocytes (panels **H and I**). Tyro3 was detected in GABAergic neurons, astrocytes and oligodendrocyte precursors as revealed by the yellow regions indicating overlap in the staining of Tyro3 and cell-type specific antibodies (panels **C**, **F** and **I)**. The staining was performed in the presence of 0.1% Triton-X 100 for all panels. Anti-Gad65, anti-GFAP and anti-O4 antibodies were labeled with secondary antibodies coupled with AlexaFluor 594 (in red) and anti-Tyro3IgFN antibodies were labeled with secondary antibodies coupled to AlexaFluor 488 (in green). Scale bar= 50 μm for **A-C**, and **G-I** and 25 μm for **D-F**.

NIH-PA Author Manuscript

NIH-PA Author Manuscript

NIH-PA Author Manuscript

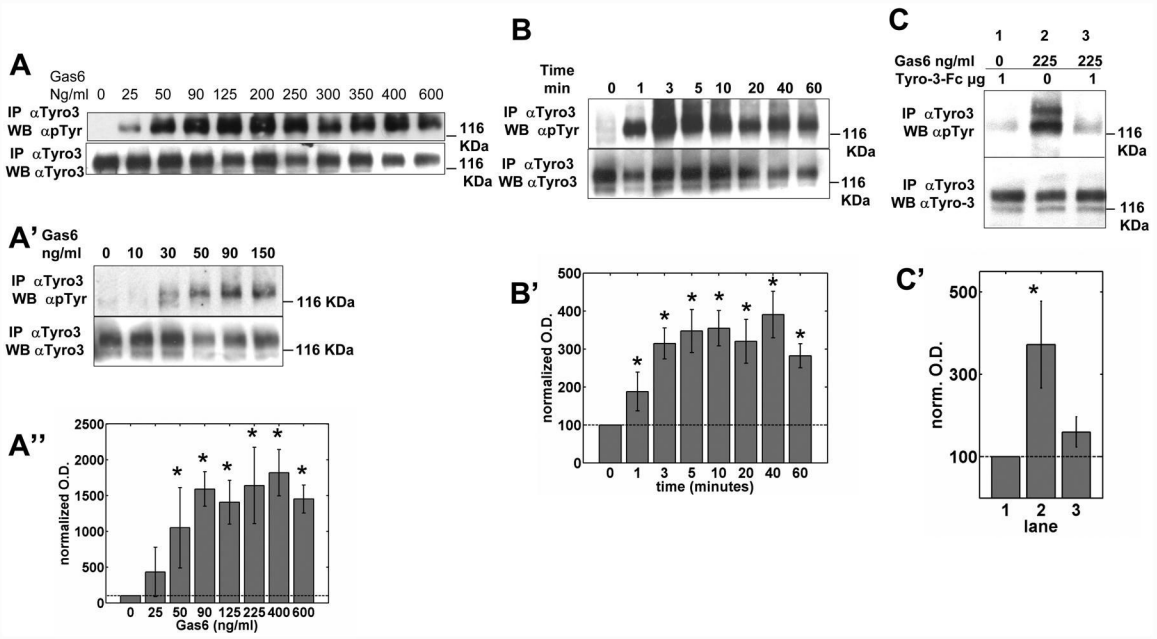

Figure 6. Characterization of Gas6 activation of Tyro3: concentration dependence and time course

Concentration dependent phosphorylation of Tyro3 in cortical neurons (**A**, **A**' and **A**''). (**A** and **A**') Representative Western blots showing the extent of Tyro3 phosphorylation upon activation with increasing amounts of Gas6. Cortical neurons were treated with Gas6 (0–600 ng/ml) for 10 min **(A)** or Gas6 (0–150 ng/ml) for 5 min **(A')** followed by cell lysis and Tyro3 immunoprecipitation (IP). SDS-PAGE using 8% gels followed by Western blot analysis was performed. The membranes were probed with anti-phosphotyrosine (α-pTyr) antibodies (PY20 and P99 mixture 1:3,500) **(A and A' Top)** and reprobed with anti-Tyro3 serum 5424 (1:3,500, α-Tyro3) **(A and A' Bottom). (A'')** Band intensities from 4 experiments were quantified by densitometric analysis and used to calculate the ratio of pTyr/5424 (total Tyro3). The bars ("normalized O.D.") represent % of control (no Gas6) which was considered 100%. * = $p<0.05$, two-tailed t-test, n = 4.

(B) Time course of Tyro3 phosphorylation by Gas6 in cortical neurons.

Representative Western blot showing the extent of Tyro3 phosphorylation after Gas6 activation (250 ng/ml) for a period spanning 1 to 60 min. Tyro3 immunoprecipitations (IPs) were performed from detergent extracts and processed for Western blotting as described in **(A).** **(B')** Band intensities from 4 experiments were quantified by densitometric analysis and used to calculate the ratio of pTyr/5424 (total Tyro3). The bars ("normalized O.D.") represent % of control (0 min time point) which was considered 100%. * = $p<0.05$, two-tailed t-test, n = 4.

(C) Tyro3-Fc receptor bodies block the ability of Gas6 to activate Tyro3.

Representative Western blot showing the extent of Tyro3 phosphorylation after Gas6 stimulation in the presence or absence of Tyro3-Fc receptor bodies. Media (0) or 225 ng/ml of Gas6 were preincubated with 1 μg Tyro3-Fc for 30 min. Cortical neurons were treated with media and 1 μg anti-Tyro3 Fcs **(lane 1)**, Gas6 225 ng/ml **(lane 2)** and Gas6 (225 ng/ml) preincubated with 1 μg Tyro3 Fcs **(lane 3**) for 10 min. Tyro3 immunoprecipitations (IPs) were performed and processed as described for **(A). (C')** Band intensities from 4 experiments were quantified by densitometric analysis and used to calculate the ratio of pTyr/5424 (total Tyro3). The bars ("normalized O.D.") represent % of control (no Gas6) which was considered 100%. * = $p<0.05$, two-tailed t-test, ** = $p<0.05$, one-tailed t-test. All comparisons for n = 3.

NIH-PA Author Manuscript

NIH-PA Author Manuscript

NIH-PA Author Manuscript

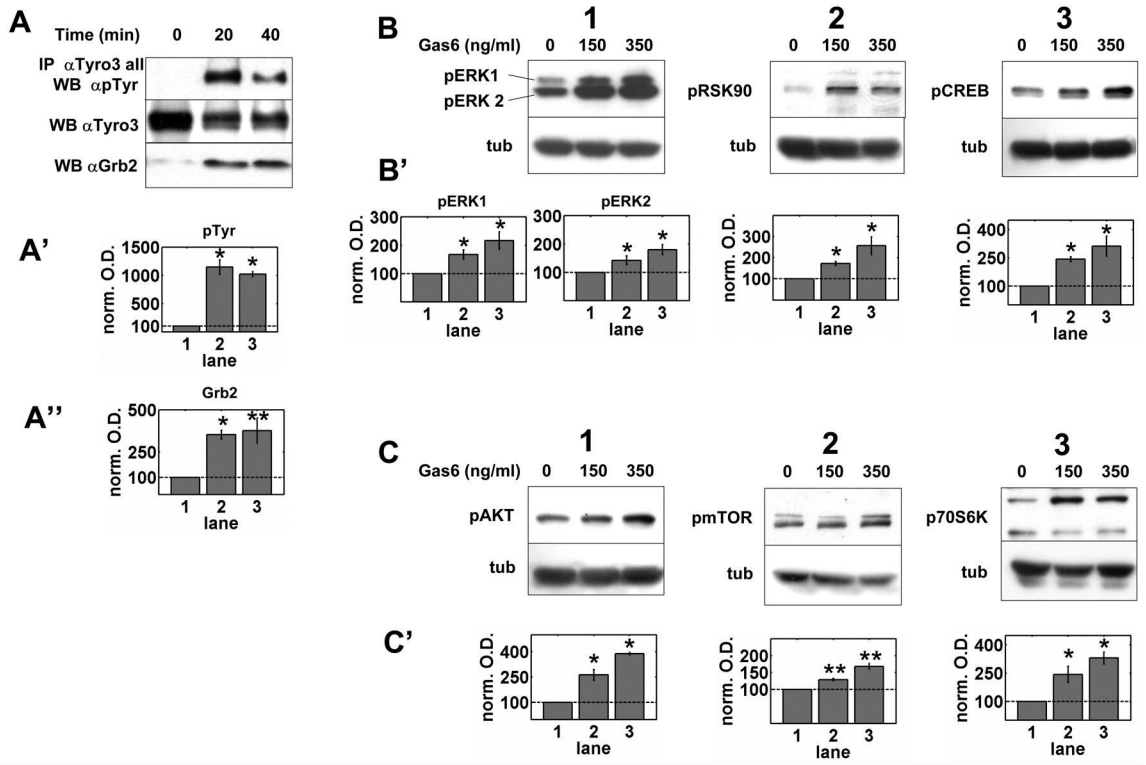

Figure 7. Gas6/Tyro3 signaling in cortical neurons: Recruitment of Grb2 and activation of the MAPK and PI(3)K signaling pathways

(A) Representative Western blot showing levels of Tyro3 phosphorylation and the association of Grb2 with Tyro3. Cortical neurons were treated with 225 ng/ml of Gas6 for 0, 20 or 40 min followed by Tyro3 immunoprecipitation (IP). After SDS-PAGE in 4–20% gels and transfer, the membranes were cut at the location of the 45 KDa marker and the top portion was probed with anti-phosphotyrosine (α-pTyr) antibodies (PY20 and P99 mixture 1:3,500) **(top)** and the bottom portion was blotted with α-Grb2 (1:500) **(bottom**). The membrane blotted against pTyr was re-probed with anti-Tyro3 serum 5424 (1:3,500, α-Tyro3) **(center). (A')** Band intensities from 3 experiments were quantified by densitometric analysis and used to calculate the ratio of pTyr/5424 (total Tyro3) the ratio of Grb2/5424 (total Tyro3). The bars ("normalized O.D.") represent % of control (no Gas6) which was considered 100%. * = $p<0.05$, two-tailed t-test, ** = $p<0.05$, one-tailed t-test. All comparisons for n = 3.

(**B** and **C**) Changes in the phosphorylation levels of Tyro3 downstream targets.
Cortical neurons were treated with 0, 150 and 350 ng/ml of Gas6 for 20 min. Normalized detergent cell extracts were separated by SDS-PAGE in 4–20% gels and blotted with antibodies directed against the MAPK signaling pathway **(B1, 2 and 3): B1** pERK1/2; **B2,** pRSK90 and **B3** pCREB. **(C)** The PI(3)K signaling pathway: **C1** pAKT, **C2** pmTOR and **C3** pp70S6kinase. The blots were reprobed with anti-tubulin III (Tuj1) shown beneath each panel as protein loading control

(B'1-3 and C'1-3). Band intensities from 3 experiments were quantified by densitometric analysis and used to calculate the ratio of **B'1** pERK1/tubulin and pERK2/tubulin, **B'2** pRSK/tubulin, **B'3** pCREB/tubulin, **C'1,** pAKT/tubulin, **C'2** pmTOR/tubulin, AND **C'3** pp70S6K/tubulin. The bars ("normalized O.D.") represent % of control (no Gas6) which was considered 100%. * = $p<0.05$, two-tailed t-test, ** = $p<0.05$, one-tailed t-test. All comparisons for n = 3.